

รูป 3.22 ความสัมพันธ์ระหว่าง  $\Delta G$ ' และความแรงสนามไฟฟ้าสำหรับฟิล์มคอมโพสิต PTh/SIS

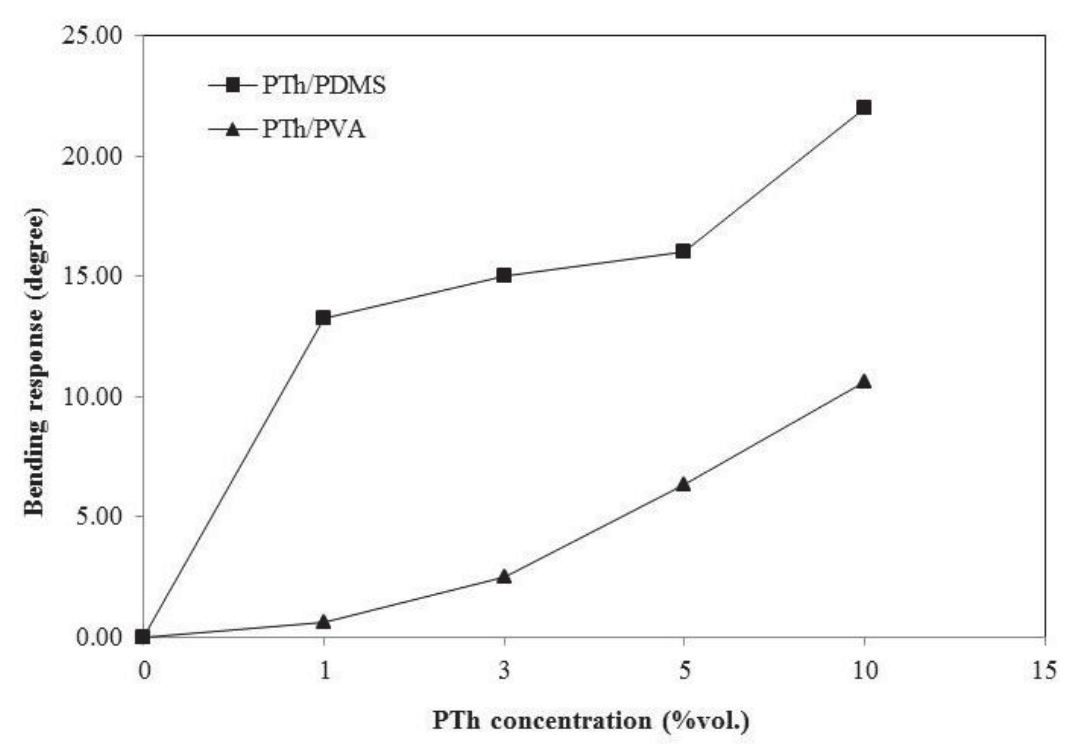
จากรูป 3.21 และ 3.22 พบว่าเมื่อความแรงของสนามไฟฟ้าเพิ่มมากขึ้นค่าการตอบสนอง ของค่ามอดูลัสสะสม (Storage modulus response,  $\Delta$ G') ของฟิล์มคอมโพสิตมีค่ามากขึ้น แสดงว่า ฟิล์มคอมโพสิตมีความแข็งแรงเพิ่มมากขึ้น เนื่องจากความแรงสนามไฟฟ้าที่เพิ่มขึ้นทำให้เกิดการ โพลาไรเซชันของโมเลกุลได้มากขึ้น ทำให้เกิดสภาพขั้วและการยึดเหนี่ยวระหว่างโมเลกุลมากขึ้น วัสดุจึงสามารถต้านทานแรงที่มากระทำได้ดีขึ้น

# 3.3.3.2 พฤติกรรมไดอิเล็กโครโฟรีติก (Dielectrophoretic behavior)

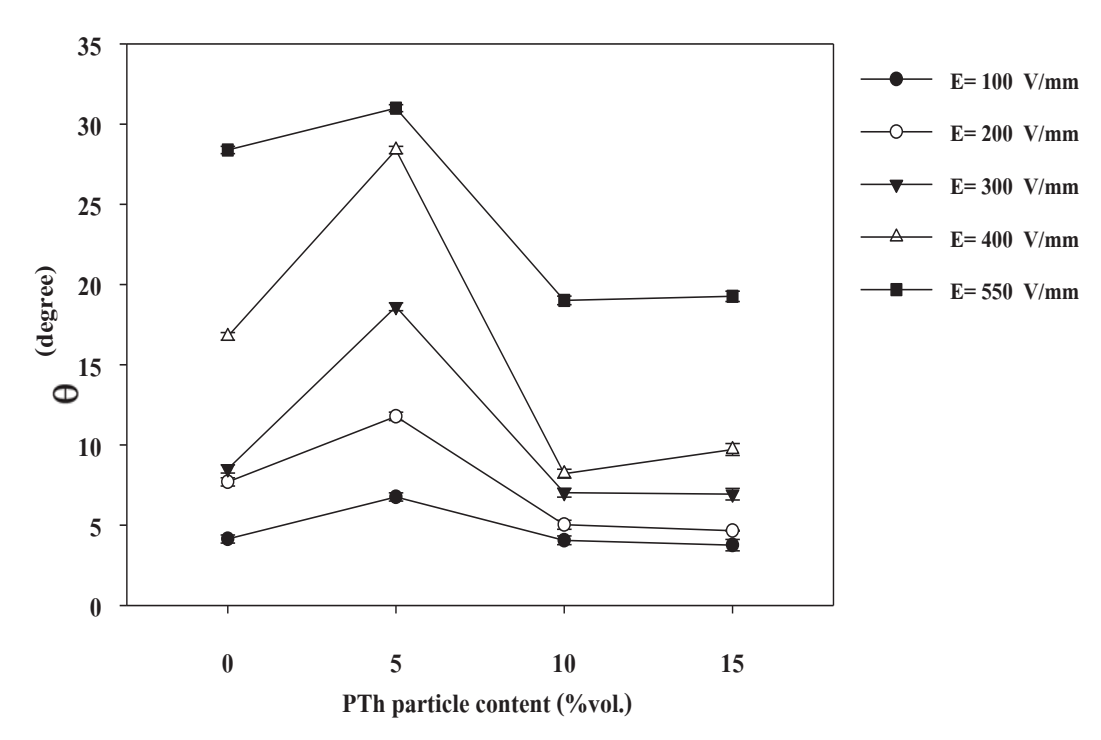
สำหรับการทดสอบการโค้งงอภายใต้กระแสไฟฟ้า (Bending response) ทำได้โดยการ เตรียมชิ้นทดสอบขนาดความกว้างประมาณ 2.0 มิลลิเมตร ยาวประมาณ 25 มิลลิเมตร หนา ประมาณ 0.5-0.7 มิลลิเมตร จากนั้นนำชิ้นทดสอบมายึดด้วยแท่นจับยึดของชุดอุปกรณ์ทดสอบการ โค้งงอภายใต้กระแสไฟฟ้า ซึ่งประกอบด้วยขั้วทองแดง 2 แผ่น ที่ต่อกับเครื่องกำเนิดไฟฟ้า กระแสตรงโดยขั้วทองแดงทั้งสองจะจุ่มในซิลิโคน (Silicone oil) ที่มีความหนืด 100 เซนติสโครก (cSt) จากนั้นจึงทำการให้กระแสไฟฟ้าที่มีความแรงในช่วง 0-700 โวลต์ต่อมิลลิเมตร พร้อมกับ บันทึกการเปลี่ยนแปลงของชิ้นทดสอบด้วยกล้องวิดีโอ แล้ววัดมุมการโค้งงอของชิ้นทดสอบโดยใช้ โปรแกรม Engauge digitizer program ผลการทดสอบเป็นดังนี้

# อิทธิพลของความเข้มข้นอนุภาคพอลิทิโอฟืน

การทดสอบอิทธิพลของความเข้มข้นอนุภาคพอลิทิโอฟินต่อมุมการโค้งงอของพอลิเมอร์ ผสม โดยใช้ความเข้มข้นของอนุภาคพอลิทิโอฟินในช่วง 0–10 เปอร์เซ็นต์โดยปริมาตร ผลการ ทดลองแสดงดังรูป 3.23-3.24



รูป 3.23 ความสัมพันธ์ระหว่างมุมการโค้งงอและความเข้มข้นอนุภาคพอลิทิโอฟิน สำหรับฟิล์มคอมโพสิต PTh/PDMS และ PTh/PVA

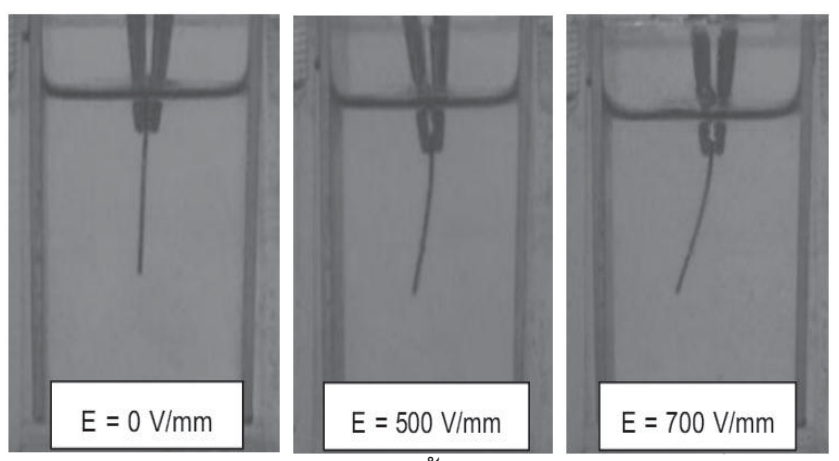


รูป 3.24 ความสัมพันธ์ระหว่างมุมการโค้งงอและความเข้มข้นอนุภาคพอลิทิโอฟิน สำหรับฟิล์มคอมโพสิต PTh/SIS

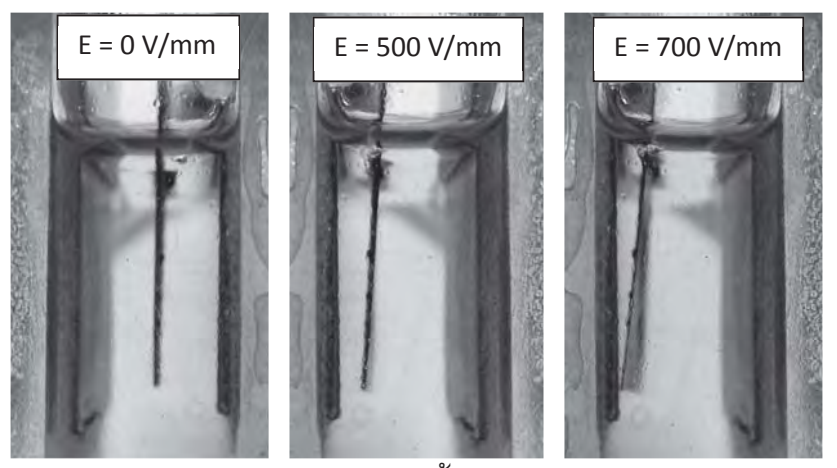
จากรูป 3.25 และ 3.26 พบว่ามุมการโค้งงอของฟิล์มคอมโพสิตที่เติมพอลิทิโอฟินมี แนวโน้มเพิ่มขึ้น เมื่อความเข้มข้นของอนุภาคพอลิทิโอฟินในฟิล์มคอมโพสิตมีค่าเพิ่มขึ้น โดยฟิล์ม คอมโพสิตสามารถตอบสนองต่อสนามไฟฟ้าได้ดี โดยสามารถโค้งงอเข้าสู่ขั้วบวก

# • <u>อิทธิพลของความแรงสนามไฟฟ้า</u>

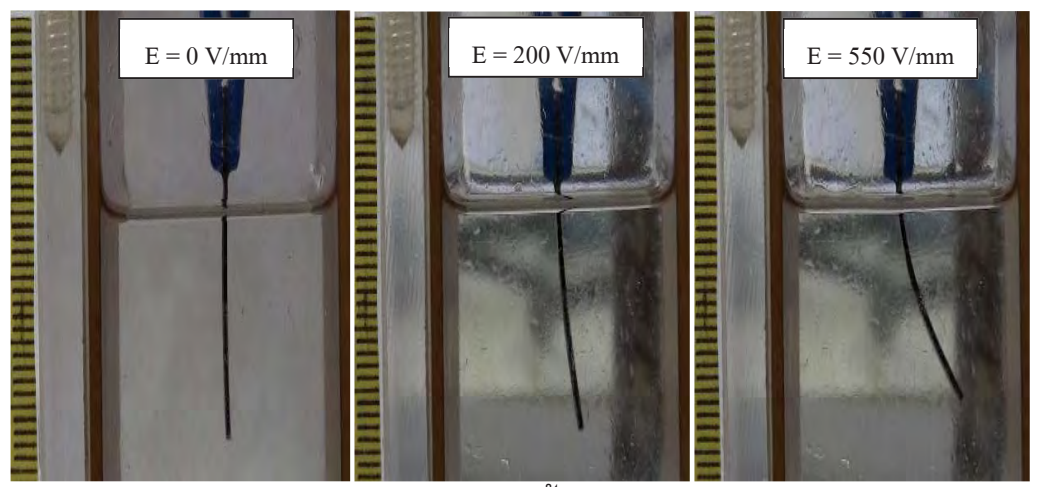
สำหรับการทดสอบอิทธิพลของความแรงสนามไฟฟ้าต่อการโค้งงอของพอลิเมอร์ผสม ได้ ทำการปรับเปลี่ยนความแรงสนามไฟฟ้าในช่วง 0–2สนาม กิโลโวลต์ต่อมิลลิเมตร ผลการทดลอง แสดงดังรูป 3.25-3.29



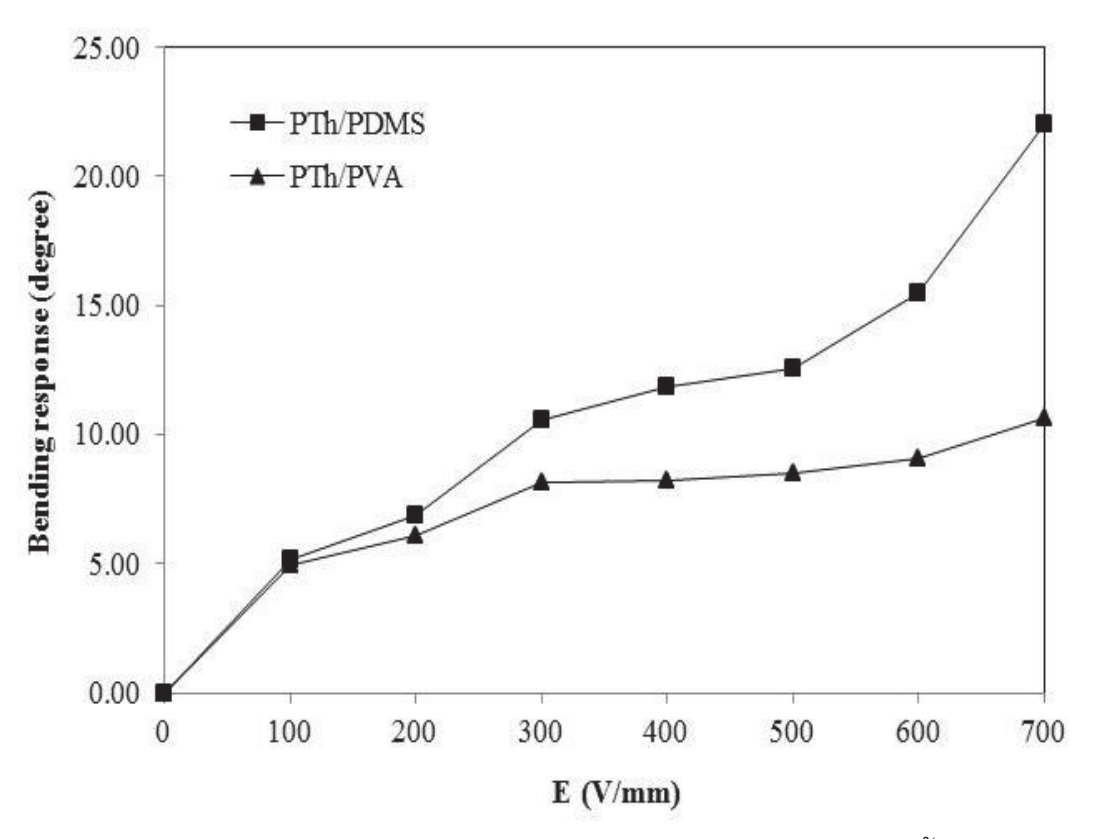
รูป 3.25 การโค้งงอภายใต้สนามไฟฟ้าของฟิล์มคอมโพสิต PTh/PDMS



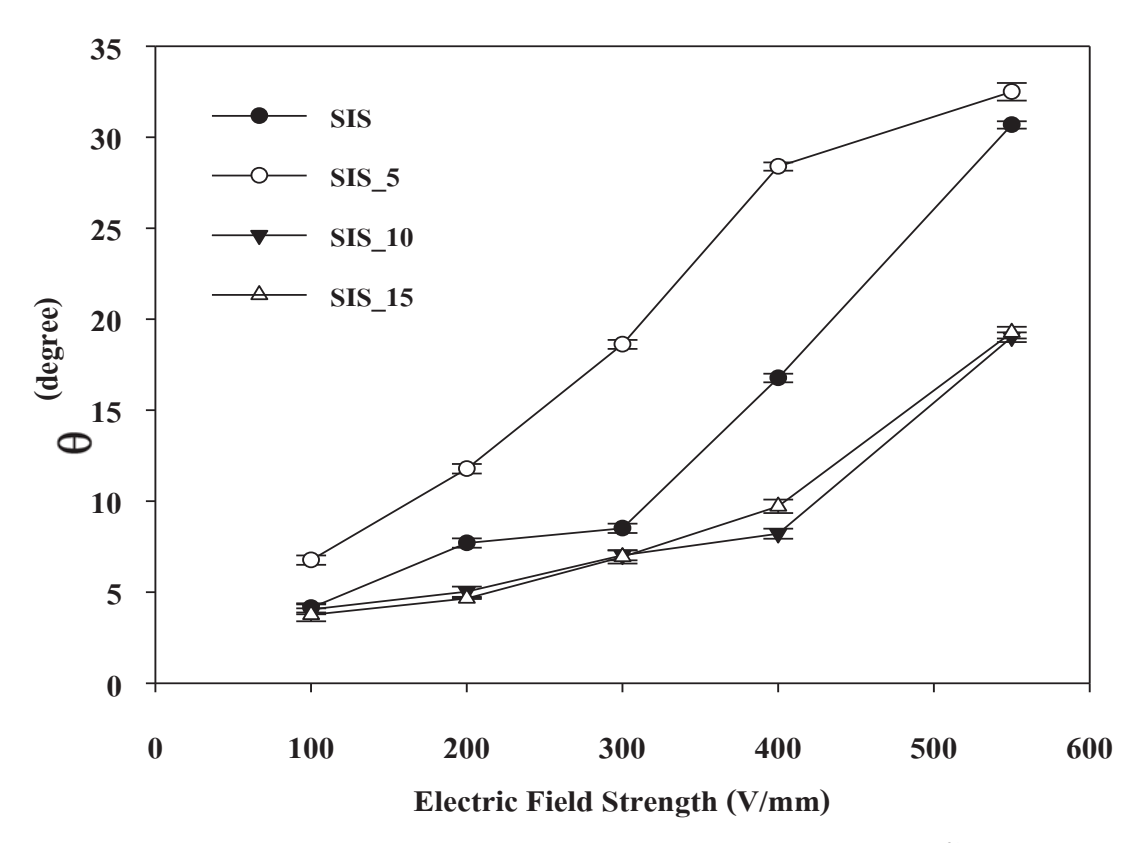
รูป 3.26 การโค้งงอภายใต้สนามไฟฟ้าของฟิล์มคอมโพสิต PTh/PVA



รูป 3.27 การโค้งงอภายใต้สนามไฟฟ้าของฟิล์มคอมโพสิต PTh/SIS



รูป 3.28 ความสัมพันธ์ระหว่างมุมการโค้งงอและความแรงสนามไฟฟ้า สำหรับฟิล์มคอมโพสิต PTh/PDMS และ PTh/PVA



รูป 3.29 ความสัมพันธ์ระหว่างมุมการโค้งงอและความแรงสนามไฟฟ้า สำหรับฟิล์มคอมโพสิต PTh/SIS

จากรูป 3.28-3.29 พบว่าเมื่อความแรงสนามไฟฟ้าเพิ่มมากขึ้นทำให้มุมการโค้งงอของ ฟิล์มคอมโพสิตมีค่าเพิ่มขึ้น เนื่องจากความแรงสนามไฟฟ้าที่เพิ่มขึ้นจะทำให้โมเลกุลของพอลิทิ โอฟินในฟิล์มคอมโพสิตเกิดการโพลาไรเซชันได้ดียิ่งขึ้นจึงเกิดสภาพขั้วได้มากขึ้น ซึ่งสภาพขั้วที่ เกิดขึ้นนี้จะทำให้มีแรงดึงดูดระหว่างขั้วของโมเลกุลในฟิล์มคอมโพสิตกับขั้วของแผ่นทองแดง อิเล็กโทรดเกิดขึ้น ซึ่งถ้าแรงดึงดูดนี้สามารถเอาชนะแรงตึงผิวระหว่างฟิล์มคอมโพสิตกับน้ำมัน ซิลิโคนได้ ก็จะทำให้เห็นการโค้งงอของฟิล์มคอมโพสิตเข้าสู่ขั้วอิเล็กโทรด

# บทที่ 4

# สรุปผลการทดลอง

# 4.1 สรุปผลการทดลอง

งานวิจัยนี้ได้ศึกษาการเตรียมฟิล์มคอมโพสิตพอลิทิโอฟิน/พอลิเมอร์ โดยใช้พอลิเมอร์ชนิด พอลิเมทิลไซลอกเซน พอลิไวนิลแอลกอฮอล์ และพอลิสไตรีน-ไอโซพรีน-สไตรีน ไตรบล็อกโคพอลิ เมอร์เป็นเมทริกซ์ โดยได้ทำการสังเคราะห์พอลิทิโอฟินด้วยวิธี Chemical oxidative polymerization โดยใช้ Iron (III) chloride เป็นตัวออกซิไดซ์ จึงเตรียมฟิล์มพอลิเมอร์คอมโพสิตและศึกษาสมบัติเชิง ไฟฟ้ากล ได้แก่ กระแสวิทยาภายใต้กระแสไฟฟ้า และการโค้งงอภายใต้กระแสไฟฟ้าของฟิล์มพอลิ เมอร์คอมโพสิต ซึ่งสามารถสรุปผลการศึกษาได้ดังนี้

## 4.1.1 สมบัติกระแสวิทยาภายใต้กระแสไฟฟ้า

การทดสอบสมบัติเชิงไฟฟ้ากลของฟิล์มพอลิเมอร์คอมโพสิตในงานวิจัยนี้ ได้ทำโดยการ ทดสอบสมบัติกระแสวิทยาภายใต้กระแสไฟฟ้า (Electrorheology) พบว่า

# - อิทธิพลของความเข้มข้นอนุภาคพอลิทิโอฟืน

ฟิล์มพอลิเมอร์คอมโพสิตที่เติมพอลิทิโอฟินมีค่าการตอบสนองของค่ามอดูลัสสะสม (Storage modulus response,  $\Delta G$ ) เพิ่มขึ้น เมื่อความเข้มข้นของอนุภาคพอลิทิโอฟินเพิ่มขึ้น

# - อิทธิพลของความแรงกระแสไฟฟ้า

เมื่อความแรงของกระแสไฟฟ้าเพิ่มมากขึ้นค่า  $\Delta G$ ' ของฟิล์มพอลิเมอร์คอมโพสิตมีค่ามาก ขึ้น

## 4.1.2 การโค้งงอภายใต้กระแสไฟฟ้า

# - <u>อิทธิพลของความเข้มข้นอนุภาคพอลิทิโอฟืน</u>

ฟิล์มพอลิเมอร์คอมโพสิตที่เติมพอลิทิโอฟินมีมุมการโค้งงอเพิ่มขึ้น เมื่อความเข้มข้นของ อนุภาคพอลิทิโอฟินเพิ่มขึ้น

# - <u>อิทธิพลของความแรงกระแสไฟฟ้า</u>

เมื่อความแรงของกระแสไฟฟ้าเพิ่มมากขึ้น มีผลทำให้มุมการโค้งงอของพิล์มพอลิเมอร์ คอมโพสิตเพิ่มขึ้น

# Output ของโครงการวิจัย

## ผลงานตีพิมพ์วารสารวิชาการระดับนานาชาติ

- [1] Thawatchai Tungkavet, Nispa Seetapan, Datchanee Pattavarakorn and Anuvat Sirivat, Improvements of eletromechanical properties of gelatin hydrogels by blending with nanowire polypyrrole: effects of electric field and temperature, (2012) Polymer International, 61, 825-833.
- [2] Thawatchai Tungkavet, Datchanee Pattavarakorn and Anuvat Sirivat, Bio-compatible Gelatins (Ala-Gly-Pro-Arg-Gly-Glu-4Hyp-Gly-Pro-) and Electromechanical properties: effects of temperature and electric field", Journal of Polymer research (2012), 19, 9759-9767.

# การนำเสนอในที่ประชุมวิชาการระดับนานาชาติ

- [1] Siripong Thongbor and <u>Datchanee Pattavarakorn</u>, "Electromechanical properties of Electroactive Polythiophene/Elastomer Blend", TIChE International Conference 2011, 10-11 November 2011, Hatyai, Songkhla, THAILAND.
- [2] D. Pattavarakorn, K. Jaitang, P. Kumchaiya, P. Chaimongkol and S. Thongbor, "Conductive Polythiophene/Polymer Composites as Electroactive Material Application", 21-26 August 2011, Jeju Island, South Korea.
- [3] Siripong Thongbor, Siriluck Chumsaratool, Sujitra Thaithed and Datchanee Pattavarakorn, "Electromechanical Properties of Conductive Polythiophene/Poly (dimethyl siloxane) Blend", The 17th Regional Symposium on Chemical Engineering, 22-23 November 2010, Bangkok, Thailand.

## เอกสารอ้างอิง

- [1] G.G. Wallace, G.M. Spinks, L. Kane-Maguire and P.R. Teasdale. Conductive Electroactive Polymers: Intelligent Materials Systems, 2nd Edition (2003), CRC Press, New York, USA.
- [2] K.C. Persaud, "Polymers for chemical sensing", Material today, 8(4) (2005), 38-44.
- [3] Responsive (smart) materials , [ระบบออนไลน์], แหล่งที่มา www.designinsite.dk (10 ตุลาคม 2554)
- [4] C. Vancaeyzeele, O. Fichet, J. Laskar, S. Boileau and D. Teyssie. "Polyisobutene/polystyrene interpenetrating polymer networks: Effects of network formation order and composition on the IPN architecture", Polymer, 47 (2006), 2046– 206.
- [5] J. S. Turner and Y. L. Cheng. "Preparation of PDMS-PMAA Interpenetrating Polymer Network Membranes Using the Monomer Immersion Method", Macromolecules, 33 (2000), 3714-3718.
- [6] G. Kofod and P. S. Larsen. "Silicone dielectric elastomer actuators: Finite-elasticity model of actuation", Sensors and Actuators A, 122 (2005), 273–283.
- [7] N.C. Goulbourne, E.M. Mockensturm and M.I. Frecker. "Electro-elastomers: Large deformation analysis of silicone membranes", International Journal of Solids and Structures, 44 (2007), 2609-2626.
- [8] L. Patrick, K. Gabor and M. Silvain. "Characterization of dielectric elastomer actuators based on a hyperelastic film model", Sensors and Actuators A, 135 (2007), 748–757.
- [9] M. Wissler and E. Mazzaa. "Mechanical behavior of an acrylic elastomer used in dielectric elastomer actuators", Sensors and Actuators A, 134 (2007), 494–504.
- [10] ElectroActive Polymers Wikipedie, the free encyclopedie, [ระบบออนไลด์]. แหล่งที่มา http://en.wikipedia.org/wiki/Electroactive\_polymers (10 พฤศจิกายน 2554)
- [11] ElectroActive Polymers–EAPs, [ระบบออนไลด์]. แหล่งที่มา www.azom.com/article.aspx?ArticleID=885 (10 พฤศจิกายน 2554)
- [12] Electrochemistry Encyclopedia -- Electroactive polymers (EAP), [ระบบออนไลด์]. แหล่งที่มา http://electrochem.cwru.edu/encycl/art-po2-elact-pol.htm (10 พฤศจิกายน 2554)
- [13] K.C. Persaud, "Polymers for chemical sensing", Material today, 8(4): 38-44 (2005).

- [14] Plastic Electronics Consortium of Thailand Conductive Polymer, [ระบบออนไลด์]. แหล่งที่มา http://nanotech.sc.mahidol.ac.th/pe-thailand/condplastic.html (20 พฤศจิกายน 2554)
- [15] J.W. Cowie, "Chemistry and Physics of Modern Materials", 2th ed., Chapman Hall, 1991.
- [16] H.R. Allcocle and F.W Lampe, "Contemporary Polymer Chemistry", 6th ed., Prentice Hall, 1996.
- [17] Electronic band structure, [ระบบออนไลด์]. แหล่งที่มา http://en.wikipedia.org/wiki/Band\_structure (24 ตุลาคม 2554)
- [18] A. Wirden, "Electroactive Polymer Materials: State of the art review of conductive polymer", 3rd ed., National Defense Research Institute Stockholm, Sweden, 1996.
- [19] D. Kumar and R.C. Sharma, "Review Article Advances in Conductive Polymers", European Polymer Journal, 34, 1053-1060 (1998).
- [20] Polythiophene Wikipedia, the free encyclopedia, [ระบบออนไลด์]. แหล่งที่มา http://en.wikipedia.org/wiki/Polythiophene (2 พฤศจิกายน 2554)
- [21] T. Puvanatvattana, D. Chotpattananont, P. Hiamtup, S. Niamlang, A. Sirivat and A.M. Jamieson. "Electric field induced stress moduli in polythiophene/polyisoprene elastomer blends", Reactives & Functional Polymer, 66 (2006), 1575-1588.
- [22] P. Thipdech, R. Kunanuruksapong and A. Sirivat. "Electromechanical responses of poly(3-thiopheneacetic acid)/acrylonitrile-butadiene rubbers", eXPRESS Polymer Letters, 2 (2008), 866- 877.
- [23] K. Thongsak, R. Kunanuruksapong, A. Sirivat, W. Lerdwijitjarud. "Electroactive polydiphenylamine/poly(styrene-block-isoprene-block-styrene)(SIS) blends: Effects of particle concentration and electric field", Materials Science and Engineering C, 31 (2011), 206-214.
- [24] P. Hiamtup, A. Sirivat and A.M. Jamieson. "Electromechanical response of a soft and flexible actuator based polyaniline particles embedded in a cross-linked poly (dimethyl siloxane) network", Materials Science and Engineering C, 28 (2008), 1044-1051.
- [25] P. Thipdech, R. Kunanuruksapong and A. Sirivat. "Electromechanical responses of poly(3-thiopheneacetic acid)/acrylonitrile-butadiene rubbers", eXPRESS Polymer Letters, 2 (2008), 866-877.

- [26] T. Puvanatvattana, D. Chotpattananont, P. Hiamtup, S. Niamlang, A. Sirivat and A.M. Jamieson. "Electric field induced stress moduli in polythiophene/polyisoprene elastomer blends", Reactives & Functional Polymer, 66 (2006), 1575-1588.
- [27] G. Han and G. Shi. "Electrochemical actuator based on single-layer polypyrrole film", Sensors and Actuator B, 113 (2006), 259-264.
- [28] W. Wichiansee and A. Sirivat. "Electromechanical properties of poly(dimethylsiloxane) and poly(3,4-ethylenedioxythiophene)/ poly(stylene sulfonic acid)/ ethylene glycol blends", Materials Science and Engineering, 29 (2009), 78-84.
- [29] R. Kunnanuruksapong and A. Sirivat. "Poly (p-phenylene) and acrylic elastomer blends for electroactive application", Materials Science and Engineering, 454-455 (2007), 453-460.
- [30] J. Lin, Q. Tang, D. Hu, X. Sun, Q. Li and J. Wu, "Electric field sensitivity of conducting hydrogels with interpenetrating polymer network structure", Colloids and Surfaces A: Physicochem. Eng. Aspects, 346 (2009), 177–183.
- [31] P. Ludeelerd, S. Niamlang, R. Kunaruksapong and A. Sirivat, "Effect of elastomer matrix type on electromechanical response of conductive polypyrrole/elastomer blends", Physics and Chemistry of Solids, 71 (2010), 1243-1250.
- [32] T. Puvanatvattana, D. Chotpattananont, P. Hiamtup, S. Niamlang, R. Kunanuraksapong, A. Sirivat and A.M. Jamieson, "Electric field induced stress moduli of polythiophene/polyisoprene suspensions: Effects of particle conductivity and concentration", Materials Science and Emgineering C, 28 (2008), 119-128.
- [33] P. Hiamtup, A. Sirivata and A.M. Jamieson, "Electrorheological properties of polyaniline suspensions: Field-induced liquid to solid transition and residual gel structure", Colloid and Interface Science, 295 (2006), 270–278.



## ผลงานตีพิมพ์ในวารสารวิชาการระดับนานาชาติ

[1] Thawatchai Tungkavet, Nispa Seetapan, Datchanee Pattavarakorn and Anuvat Sirivat, Improvements of eletromechanical properties of gelatin hydrogels by blending with nanowire polypyrrole: effects of electric field and temperature, (2012) Polymer International, 61, 825-833.

#### Research Article



Received: 1 September 2011

Revised: 1 November 2011

Accepted: 1 November 2011

Published online in Wiley Online Library: 30 January 2012

(wileyonlinelibrary.com) DOI 10.1002/pi.4149

# Improvements of electromechanical properties of gelatin hydrogels by blending with nanowire polypyrrole: effects of electric field and temperature

Thawatchai Tungkavet,<sup>a</sup> Nispa Seetapan,<sup>b</sup> Datchanee Pattavarakorn<sup>c</sup> and Anuvat Sirivat<sup>a</sup>\*

#### Abstract

Nanowire-polypyrrole/gelatin hydrogels were fabricated by dispersion of nanowire-polypyrrole into a gelatin aqueous solution followed by solvent casting. The electromechanical properties, thermal properties and deflection of pure gelatin hydrogel and nanowire-polypyrrole/gelatin hydrogels were studied as functions of temperature, frequency and electric field strength. The 0.01%, 0.1%, 0.5%, 1% v/v nanowire-polypyrrole/gelatin hydrogels and pure gelatin hydrogel possess storage modulus sensitivity values of 0.75, 1.04, 0.88, 0.99 and 0.46, respectively, at an electric field strength of 800 V mm<sup>-1</sup>. The effect of temperature on the electromechanical properties of the pure gelatin hydrogel and nanowire-polypyrrole/gelatin hydrogels was investigated between 30 and 80 °C; there are three regimes for the storage modulus behaviour. In deflection testing in a cantilever fixture, the dielectrophoresis force was determined and found to increase monotonically with electric field strength. The pure gelatin hydrogel shows the highest deflection angle and dielectrophoresis force at an electric field strength of 800 V mm<sup>-1</sup> relative to those of the nanowire-polypyrrole/gelatin hydrogels.

Keywords: biopolymer; gelatin; hydrogels; conducting polymers; actuator

#### INTRODUCTION

The exchange of electrical energy and mechanical energy has been of scientific and technological interest for many decades. Electroactive polymers offer promising and novel characteristics such as light weight, high energy density and high flexibility. They are also candidates for muscle-like actuator materials. Some of the currently available materials are ionic polymer—metal composites,<sup>1</sup> gel polymers,<sup>2</sup> conductive polymers,<sup>3</sup> electric field activated electroactive polymers such as electron irradiated polyvinylidene fluoride trifluoroethylene polymers,<sup>4</sup> dielectric elastomers,<sup>5</sup> electrostrictive polymer artificial muscle<sup>6,7</sup> and electro-rheological fluids.<sup>8</sup> The development of electroactive materials for artificial muscles or actuators is sought after because of the benefits they offer.

Gelatin is one type of electroactive polymer; it is a protein biopolymer derived from the partial hydrolysis of native collagens, the most abundant structural proteins found in the animal body: skin, tendons, cartilage and bone. It is a good film- and particle-forming material. Due to its many merits – its biological origin, non-immunogenicity, biodegradability, biocompatibility and commercial availability at relatively low cost – gelatin has been widely used in the pharmaceutical and medical fields as sealants for vascular prostheses, carriers for drug delivery, wound dressings and artificial muscles. Normally gelatin is produced by denaturing a naturally derived collagen in solution through either an acidic or alkaline process in which the triple-helix structure is separated into a random coil structure. During the gelling process,

the random coil in a warm aqueous solution will change into a coil—helix structure when cooled. <sup>11</sup> However, gelatin exhibits poor mechanical properties, which limits its possible application as a biomaterial. In order to use this material in practical applications, the structure needs to be reinforced either through crosslinking or by using some filler materials. However, the presence of residual crosslinking agents can lead to toxic side effects. The use of multiwall carbon nanotubes as a reinforcement in gelatin has been studied by Haider et al. <sup>12</sup> Recently, the insertion of a conductive polymer into a biopolymer forming a blend has been of keen interest. Conductive polymers can offer a variety of benefits to the host biopolymer: variable conductivity and better thermal stability and mechanical properties. <sup>13</sup> On the other hand, conducting polymers have been intensively studied for their one-dimensional conjugated structures and adjustable conductivity. <sup>14</sup>

- \* Correspondence to: Anuvat Sirivat, Conductive and Electroactive Polymers Research Unit, Petroleum and Petrochemical College, Chulalongkorn University, Soi Chula 12, Phyathai Rd, Bangkok 10330, Thailand. E-mail: anuvat.s@chula.ac.th; www.cepru.research.ac.th
- a Petroleum and Petrochemical College, Chulalongkorn University, Bangkok 10330, Thailand
- b National Metal and Materials Technology Center, Pathumthani 12120, Thailand
- Department of Industrial Chemistry, Faculty of Science, Chiang Mai University, Chiangmai 50200. Thailand

T Tungkayet et al.

55



Among the conducting polymers, polypyrrole (Ppy) is one of the most investigated due to its high electrical conductivity, relatively good environmental stability and low toxicity. <sup>15–17</sup> Also, the synthesis of nanoscale materials has attracted great interest during the past 10 years. Chemical oxidation polymerization is simple and cheap in producing large quantities of nanostructural Ppy, because it overcomes the limitation of electrochemical polymerization. Duchet et al. <sup>18</sup> used commercial polycarbonate nanoporous particle track-etched membranes as templates to prepare Ppy nanotubules and nanofibrils.

In the present study, we were interested in blending nanowire-polypyrrole (nanowire-Ppy) as a conductive polymer with a gelatin hydrogel containing an ionic surfactant (i.e. dodecylbenzene sulfonic acid (DBSA) dispersed in an aqueous solvent). The mechanical properties, electromechanical properties and electrical properties were investigated in terms of nanowire-Ppy concentration, electric field strength and temperature.

#### **MATERIALS AND METHODS**

#### Material

Gelatin (type B, bovine skin), pyrrole monomer (Sigma) and calcium hydride (Fluka) were used as received. Anhydrous iron(III) chloride (Riedel-de Hean) was used as an oxidant without further purification. DBSA (Sigma) was used as received as a dopant.

#### Synthesis of nanowire-polypyrrole

In this work, we followed the chemical synthesis procedure of He et al. 19 for the nanowire-Ppy. The pyrrole monomer was dried by mixing with CaH2 in a ratio of 100 g of CaH2 per litre of pyrrole and the reaction was allowed to proceed for 24 h. Then 0.0175 mol DBSA and 0.0175 mol of dried pyrrole monomer were dissolved in separate beakers of 250 mL of distilled water. The solutions were mixed together by vigorously stirring to obtain an emulsion. A solution of FeCl<sub>3</sub> (0.065 mol, 0.01625 mol L<sup>-1</sup>) in deionized water was added to the emulsion at 0°C for a duration of 40 h. It was terminated by pouring a large excess of methanol into the solution. The resulting Ppy precipitate was vacuum filtered and washed with methanol, acetone and distilled water several times until the pH was equal to 6.0. Finally, it was dried in a vacuum oven for 40 h at 30 °C. Other Ppys were synthesized with the same procedure but with 0.000175, 0.00175, 0.175, 0.875 and 1.75 mol DBSA.

#### Preparation of the nanowire-polypyrrole/gelatin hydrogel

The various concentrations of nanowire-Ppy (0.01%, 0.1%, 0.5% and  $1\% \, v/v)$  were dispersed by a transonicator (Elma, D 7284) in

an aqueous medium filled with  $4\times10^{-3}$  mol L<sup>-1</sup> DBSA. Then the gelatin hydrogel was prepared by dissolution in 10% v/v distilled water (pH 6.40) at 40 °C overnight by magnetic stirring until the pH was equal to 6.31. The two solutions were mixed and poured onto a Petri dish for the hydrogel casting at room temperature. The thickness of the hydrogel samples was about 1.4 mm. Figure 1 shows a schematic diagram for the possible interaction of the gelatin and DBSA.

#### Characterization and testing of composite hydrogels

Each Ppy sample was identified for functional groups by Fourier transform infrared spectroscopy (FTIR) (Thermo Nicolet, Nexus 670) operated in the absorption mode with 32 scans and a resolution of  $\pm 4\,\mathrm{cm^{-1}}$ , covering a wavenumber range from 3500 to 500 cm $^{-1}$  using a deuterated triglycine sulfate detector. Optical grade potassium bromide (Carlo Erba reagent) was used as the background material.

Electrical conductivity was measured with a meter which consisted of two probes that made contact with the surface of the film sample. The probes were connected to a source meter (Keithley, Model 6517A) for a constant voltage source and for reading the current. The applied voltage and the resultant current in the linear ohmic regime were used to determine the electrical conductivity of the polymer using the equation

$$\sigma = \frac{1}{\rho} = \frac{1}{R_s t} = \frac{1}{KVI} \tag{1}$$

where  $\sigma$  is the specific conductivity (S cm<sup>-1</sup>),  $\rho$  is the specific resistivity ( $\Omega$  cm),  $R_s$  is the sheet resistivity ( $\Omega$ ), l is the measured current (A), K is the geometric correction factor, V is the applied voltage (V) and t is the pellet thickness (cm).

Scanning electron micrographs were taken with a scanning electron microscope (JEOL, model JSM-5200) to determine the morphology of the Ppy in powder form at various DBSA concentrations. The micrographs of Ppy were obtained by using an acceleration voltage of 15 kV with magnifications of 15 000 and 100 000 times.

AFM (CSPM 4000) images were taken with a scanning electron microscope to determine the topology of the hydrogels at various concentrations of nanowire-Ppy by using a scan rate 0.5 Hz and a scan size of  $10 \, \mu m \times 10 \, \mu m$ .

A melt rheometer (Rheometric Scientific, ARES) was used to measure the rheological properties. It was fitted with a custom-built copper parallel plate fixture (diameter 30 mm). A DC voltage was applied with a DC power supply (Instek, GFG8216A), which can deliver an electric field strength to 800 V mm<sup>-1</sup>. A digital multimeter was used to monitor the voltage input. In these

Figure 1. Scheme of the possible interaction of the gelatin and DBSA.



experiments, the oscillatory shear strain was applied and the dynamic moduli (G' and G") were measured as functions of frequency and electric field strength. Strain sweep tests were first carried out to determine suitable strains to measure G' and G" in the linear viscoelastic regime. The appropriate strain was determined to be 0.15% for both the pure gelatin hydrogels and the nanowire-Ppy/gelatin hydrogels. Then frequency sweep tests were carried out to measure G' and G'' for each sample as functions of frequency. The deformation frequency was varied from 0.1 to 100 rad s $^{-1}$ . Before each measurement, pure gelatin hydrogels and nanowire-Ppy/gelatin hydrogels were pre-sheared at a low frequency (0.039811 rad s-1), and then the electric field was applied for 15 min to ensure the formation of equilibrium polarization before taking the G' and G" measurements. Experiments were carried out at a temperature of 30°C and repeated at least two to three times. The effect of temperature was studied at various temperatures between 30 and 80 °C for the pure gelatin hydrogels and the nanowire-Ppy/gelatin hydrogels. The temporal response experiments were carried out at 800 V mm<sup>-1</sup>. Deflections of the pure gelatin hydrogel and the nanowire-Ppy/gelatin hydrogels were carried out under various applied electric field strengths. For each hydrogel, one end of the sample was fixed with a grip vertically in a transparent chamber containing two parallel electrodes. The input DC field was provided by a DC power supply (Gold Sun 3000, GPS 3003D) and a high voltage power supply (Gamma High Voltage, UC5-30P), which delivered various electric field strengths from 25 to 600 V mm<sup>-1</sup>. A digital video recorder (Sony, Handicam HR1) was used to record the displacement of the films. The tip displacement was measured and calculated from a Scion Image (Beta 4.0.3) program.

From the static force balance, the deflecting force or the dielectrophoresis force ( $F_d$ ) on the samples is equal to the sum of the resisting elastic force (Fe) and the weight along the bending direction (Eqn (2)), where the film deflection distance at equilibrium is d.

$$F_{\rm d} = F_{\rm e} + mg \sin \theta \tag{2}$$

where m is the sample's mass (kg), g is the gravity constant (9.8 m s<sup>-2</sup>),  $\theta$  is the deflection angle and  $F_e$  is the resisting elastic force (N). In our experiment, the film deflections were small. The linear deflection theory of one free-end film was therefore used where the elastic force can be calculated using the equation 20,21

$$F_{e} = \frac{dEI}{I^{3}}$$
(3)

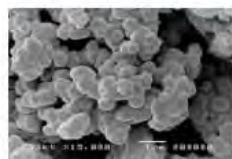
where E is the elastic modulus which is equal to  $2G'(1 + \nu)$  in which  $G'(1 \text{ rad s}^{-1}, E)$  is the shear modulus and v is Poisson's ratio, equal to 1/2 for an incompressible material, I is the moment of inertia, equal to  $t^3w/12$ , where t is the sample thickness and w is the sample width, d is the deflection distance and I is the sample

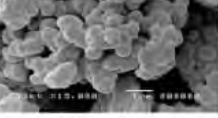
#### RESULTS AND DISCUSSION

#### Characterization of nanowire-polypyrrole

An FTIR spectrum of the Ppy was taken to identify the characteristic absorption peaks, as shown in Table 1; the characteristic peaks of the synthesized Ppy are at 1547, 1450, 1302, 1178, 1038 and  $633\,\mathrm{cm}^{-1}$ . The pyrrole ring vibration occurs at 1547 and  $1450\,\mathrm{cm}^{-1}$ ,  $^{19}$  the  $-\mathrm{C-H}$  in-plane vibration at 1302 and 1038 cm<sup>-1</sup>, <sup>19</sup> and the C-N stretching vibration at 1178 cm<sup>-1</sup>. <sup>22</sup>

Table 1. FTIR characteristic peaks of synthesized Ppy			
Wavenumber (cm <sup>-1</sup> )	Assignment		
1547, 1450	Pyrrole ring		
1302, 1038	—C−H in plane		
1178	C-N stretching		
633	Sulfonate anion		







(a) 0,00175 mol DBSA = (0.01:1)

(b) 0.175 mol DBSA



(c) 1.75 mol DBSA  $(N_{DBSA}:N_{monomer} = 10:1)$ 

Figure 2. SEM micrographs of DBSA-doped synthesized Ppy at various DBSA concentrations with a magnification of 15000 (a) 0.0175 mol ( $N_{DBSA}:N_{monomer}=0.01:1$ ); (b) 0.175 mol ( $N_{DBSA}:N_{monomer}=1:1$ ); (c) 1.750 mol ( $N_{DBSA}:N_{monomer}=1:1$ );

When Ppy is doped with DBSA, the peak at 633 cm<sup>-1</sup> increases. This peak represents the S=O and S-O stretching vibrations of sulfonate anions which compensate for the positive charges in the Ppy chains.<sup>23</sup>

The effect of the doping level on the morphology of the conductive polymer was investigated by SEM. Figure 2 shows micrographs of synthesized Ppy with various DBSA concentrations: 0.00175 to 1.75 mol (NDBSA: Nmonomer to 0.01:1, 1:1, and 10:1). It is interesting to observe that upon increasing the dopant level the morphology of the conductive polymer changes from having a typical three-dimensional random coil nanogranular structure to a nanowire fibrillar structure and then returns to a nanogranular structure again (Figs 2(a)-2(c)). The micrographs suggest that as the dopant concentration increases more polarons and bipolarons are generated along the polymer chains and they induce a granule-to-nanowire transition. It can be seen that the concentration of DBSA strongly affects the morphology of the Ppy obtained. When the concentration of DBSA in the reaction solution is higher than 0.175 mol, the resulting morphology of Ppy is granular, similar to that of Ppy synthesized with other dopants.<sup>23–25</sup> As previously mentioned, the nanowire-Ppy is obtained when the reacting solution is at a proper reactant concentration, and nanogranular Ppy is obtained with a higher reactant concentration.<sup>26</sup> The resulting Ppy average particle sizes for various DBSA concentrations (N<sub>DBSA</sub> : N<sub>monomer</sub> equal to 0.01:1, 0.1:1, 0.5:1, 1:1, 5:1 and 10:1) are tabulated in Table 2. Figure 3 shows micrographs of the cross-sections of the

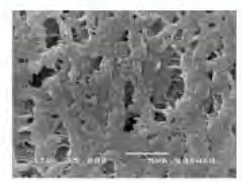
www.soci.org



SCI



gelatin



(b) Cross-section of nanowire PPy0.1 %v/v / gelatin



(c) Cross-section nanowire PPy1 %v/v / gelatin

Figure 3. SEM micrographs of cross-sections of the pure gelatin and the nanowire-Ppy/gelatin hydrogels: (a) cross-section of the pure gelatin; (b) cross-section of the 0.1 vol% nanowire-Ppy/gelatin; and (c) crosssection of the 1 vol% nanowire-Ppy/gelatin.

nanowire-Ppy/gelatin hydrogels at various nanowire-Ppy concentrations. The nanowire-Ppy shows a moderate dispersion in the gelatin solution at low nanowire-Ppy concentrations with the aid of the surfactant; the dispersion becomes relatively poor at high nanowire-Ppy concentrations. Partially homogeneous nanowire-Ppy/gelatin hydrogel is obtained due to the poor nanowire-Ppy dispersion as a result of the van der Waals forces between Ppy nanowires.

The specific electrical conductivity of Ppy and nanowire-Ppy was measured with a custom-built two-point probe (Keithley, Model 6517A). The specific electrical conductivity with corresponding standard deviations of Ppy, at  $N_{\rm DBSA}$ :  $N_{\rm monomer}$  equal to 0.01:1, 0.1:1, 0.5:1, 1:1, 5:1 and 10:1, is shown in Table 2. The electrical conductivity of Ppy is thus closely related to its morphology. The conductivity of Ppy is expressed as  $\sigma = ne\mu$  where n is the density of charge carriers, e represents the electron charge and  $\mu$  is the mobility of the charge carriers. Thus, the electrical conductivity of Ppy is proportional to the density (the doping level in the case of conducting polymers) and the mobility of the charge carriers. The conductivity of nanogranular Ppy (10:1) is 15.95 c cm<sup>-1</sup>, lower than that of nanowire-Ppy (1:1) which is 23.86 c cm<sup>-1</sup>. Ppy with nanowire morphology presumably has a higher mobility for the

charge carriers than granular Ppy and this factor dominates the charge carrier density factor.<sup>27</sup>

The topology and the orientation of the nanowire-Ppy/gelatin hydrogels were also investigated by AFM. The AFM micrographs of the nanowire-Ppy/gelatin and the pure gelatin hydrogels are demonstrated in Figs 4(a) –4(c). Figure 4(a) shows the topology and the orientation of the 0.1% v/v nanowire-Ppy/gelatin hydrogel; it consists of nanorods which are aligned in one direction with a uniform distribution by a mechanical force; the schematic diagram is illustrated in Fig. 4(a'). The 1% nanowire-Ppy/gelatin hydrogel possesses a cottage-like topology is aggregation of conductive polymer. Its topology presumably consists of nanowires piling up randomly on each other as shown in Fig. 4(b) and in the schematic diagram in Fig. 4(b') due to the agglomeration. The topology of the pure gelatin hydrogel is shown in Fig. 4(c). Figure 4(a) of the 0.1% v/v nanowire-Ppy/gelatin hydrogel shows that the nanowire-Ppy is dispersed quite uniformly within the gelatin hydrogel.

#### **Electromechanical properties**

Time dependence of the electro-rheological response

We investigated the temporal characteristics of the pure gelatin and the nanowire-Ppy/gelatin hydrogels (0.1% and 1% v/v) at an electric field strength of 800 V mm<sup>-1</sup> from the time sweep tests, in which the electric field was turned on and off alternately. The temporal characteristic of each sample was recorded in the linear viscoelastic regime at a strain of 0.15% and a frequency of 100 rad s<sup>-1</sup>. Figure 5 shows a comparison of the storage modulus G' of the pure gelatin and of the nanowire-Ppy/gelatin hydrogels during the time sweep tests. At an electric field strength of 800 V mm-1, G' immediately increases and rapidly reaches a steady-state value. For the pure gelatin hydrogel, when the electric field is turned off, G' decreases instantaneously to its original state. For the nanowire-Ppy/gelatin hydrogel (0.1% and 1% v/v), G' decreases but does not recover its original value. This behaviour indicates that there are some irreversible agglomerations of the nanowire-Ppy or some dipole moment residues, possibly due to some hydrogen bonding between adjacent nanowire-Ppy. However, the 1% v/v nanowire-Ppy/gelatin hydrogel shows a quick response under an electric field since the agglomeration of nanowire-Ppy in hydrogels constitutes large induced dipole moment domains.

#### Effect of electric field strength and concentration

The effect of electric field strength on the electromechanical properties of the nanowire-Ppy/gelatin hydrogels of 0, 0.01, 0.1, 0.5 and 1 vol% were investigated in the range 0-800 V mm<sup>-1</sup>. Figure 6 shows the storage modulus response ( $\Delta G'$ ) of the hydrogels versus electric field strength at a frequency of 100 rad s strain of 0.15% and a temperature of 30°C. The increases in  $\Delta G'$  with electric field strength are nonlinear within the range 0.1-800 V mm<sup>-1</sup>. The storage modulus response values of these samples at an electric field strength of 800 V mmare 250 000, 503 000, 1 005 000, 212 990 and 202 779 Pa for the pure gelatin, the nanowire-Ppy(0.01 vol%)/gelatin, the nanowire-Ppv(0.1 vol%)/gelatin, the nanowire-Ppv(0.5 vol%)/gelatin and the nanowire-Ppy(1 vol%)/gelatin hydrogels, respectively. (The storage modulus sensitivity values of these samples at an electric field strength of 800 V mm<sup>-1</sup> are tabulated in Table 3.) The mixing of the nanowire-Ppy into gelatin leads to increases in G' with and without an electric field. The increase of  $G_o'$  can be attributed to the effect of particles acting as fillers. For the small amount



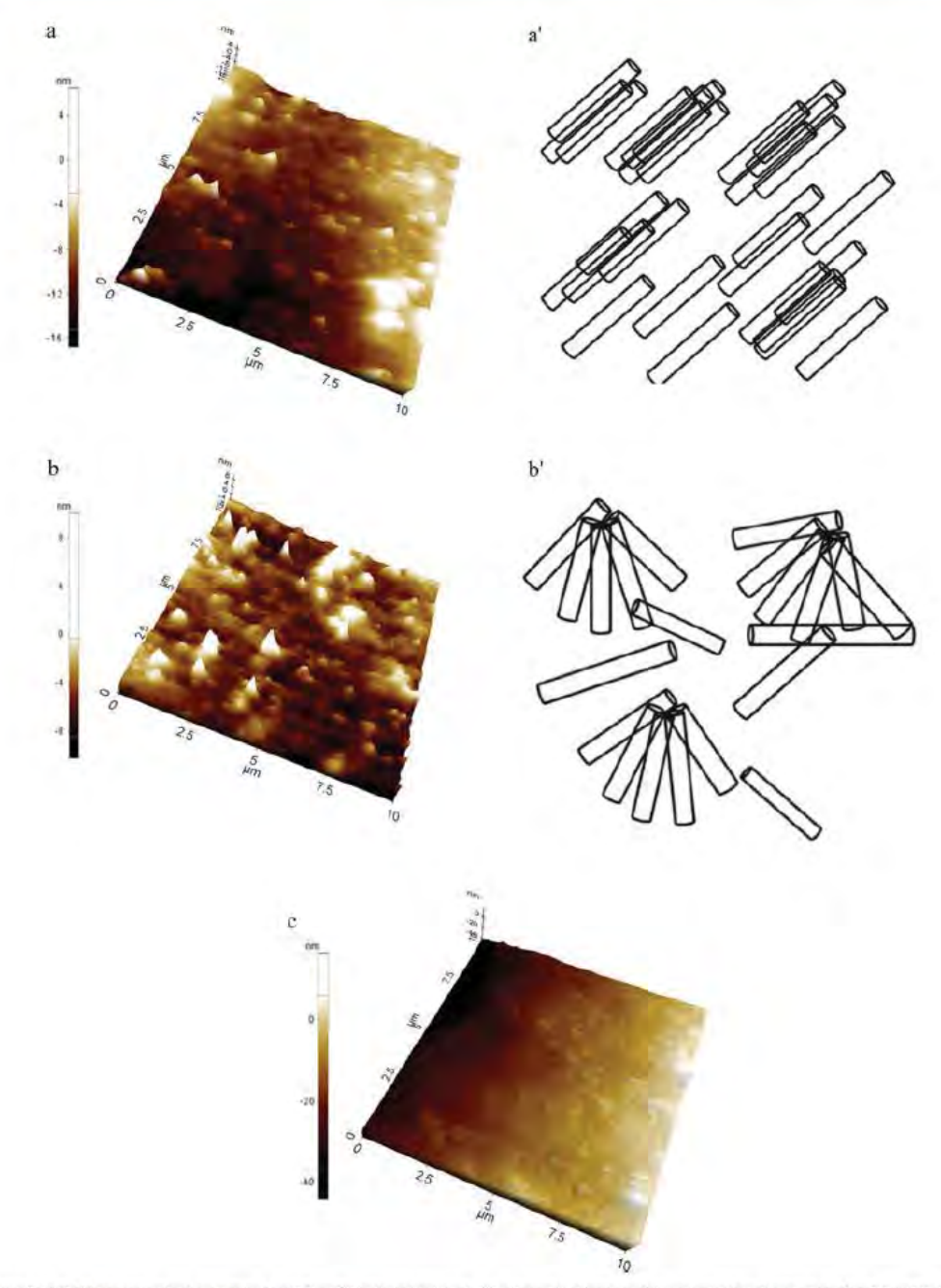


Figure 4. (a) AFM micrograph of nanowire-Ppy(0.1 vol%)/gelatin hydrogel; (a') schematic diagram of the orientation of nanowire-Ppy(1 vol%); (b) AFM micrograph of nanowire-Ppy(1 vol%)/gelatin hydrogel; (b') schematic diagram of the orientation of nanowire-Ppy(1 vol%); (c) AFM micrograph of pure gelatin hydrogel.

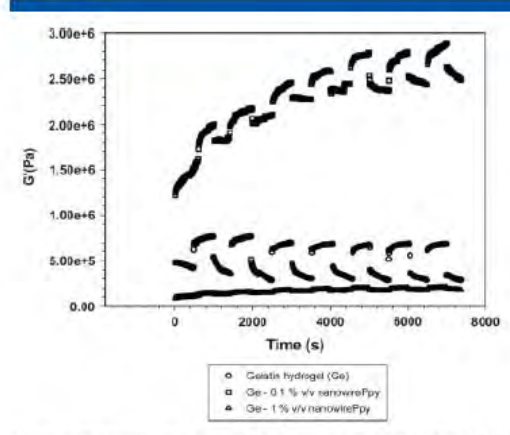


Figure 5. Temporal responses of the storage modulus (*G*′) of the pure gelatin hydrogel and the nanowire-Ppy/gelatin hydrogels (sample diameter 30 mm, gel thickness 1.405 mm, 0.15% strain, frequency 100 rad s⁻¹, electric field strength 800 V mm⁻¹, 30 °C): O, pure gelatin hydrogel; □, 0.1 vol% nanowire-Ppy, ∆, 1 vol% nanowire-Ppy.

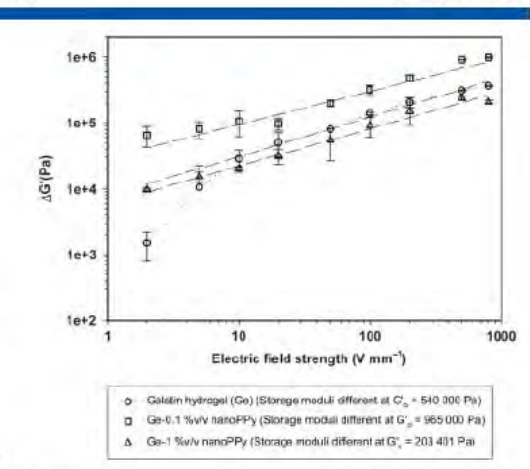


Figure 6. Effect of concentration of particles on the storage modulus response ( $\Delta G$ ) at various electric field strengths (sample diameter 30 mm, gel thickness 1.405 mm, 0.15% strain, frequency of 100 rad s<sup>-1</sup>, 30 °C): o, pure gelatin hydrogel;  $\square$ , 0.1 vol% nanowire-Ppy,  $\square$ , 1 vol% nanowire-Ppy.

of nanowire-Ppy added, the fillers induce only an additional free volume, but the distances between particles are large enough to create a significant particle interaction through the electric-field-induced dipole moments. Therefore, the storage modulus sensitivity becomes high only at suitable nanowire-Ppy concentrations. The maximum  $\Delta G'$  and  $\Delta G'/G'_{o}$  occurs with the nanowire-Ppy(0.1 vol%)/gelatin hydrogel. However, the storage modulus response and sensitivity decrease with a nanowire-Ppy concentration greater than 0.1 vol%. For the hydrogel system with the highest particle concentration of 1 vol%, the storage modulus response under the effect of the electric field diminishes since the hydrogel presumably involves phase separation between the gelatin hydrogel and the nanowire-Ppy agglomeration.

Liu and Shaw<sup>29</sup> reported a similar effect for a silica/silicone system. The enhancement of the shear modulus was negligible below 8.0 vol% but increased dramatically above this threshold concentration. Above 55 vol%, the shear modulus decreased since the interparticle force decreased with the steric hindrance effect. Kunanuruksapong and Sirivat<sup>30</sup> found that the storage modulus of a polymer blend between poly(p-phenylene) and an acrylic elastomer increased with increasing poly(p-phenylene) concentration. However, at the higher particle concentration of 30 vol%, the storage modulus response ( $\Delta G_{2kV,mm}$ ) decreased.

#### Effect of the operating temperature

The mechanical properties of the pure gelatin and the nanowire-Ppy/gelatin hydrogels in an electric field were investigated at operating temperatures between 30 and 80 °C. G' and AG' (100 rad s-1) are plotted against temperature in Fig. 7. One sample was used for each of the  $G'_o$  and G' measurements. An electric field was first applied on another sample for a period of 10 min before G' was measured successively at each temperature. Experiments were carried out using two representative hydrogels. pure gelatin and nanowire-Ppy(0.1 vol%)/gelatin hydrogel, as shown in Fig. 7. Figure 7 shows that the storage modulus of the pure gelatin hydrogel initially decreases in the temperature range 30–40  $^{\circ}$ C because of the denaturation of the triple-helix coil to a random coil.  $^{31}$  In the temperature range 40–60  $^{\circ}$ C, the storage modulus increases, consistent with classical network theory.<sup>20</sup> The higher temperature induces more entropy of the gel, leading to an increase in the retractive force and the storage modulus. However, the storage modulus decreases with increasing temperature between 60 and 80 °C, the temperature range close to the low temperature glasss transition of 120  $^{\circ}$ C in which the devitrification of  $\alpha$ -amino acid block occurs.<sup>32</sup> In the case of 0.1% nanowire-Ppy/gelatin hydrogel, the temperature increment under an electric field retards the denaturation temperature (30-40 °C) and the low temperature glass transition (60-80 °C) because of the polarization of Ppy. In addition, the storage modulus

Material (nanowire-Ppy			Sensitivity of storage		
diameter 95 ± 18 nm)	Storage modulus (G') (Pa)	Initial storage modulus $(G'_0)$ (Pa)	modulus ( $\Delta G'/G'_0$ ) (Pa)		
Gelatin hydrogel (Ge)	790 000	540 000	0.46		
Ge-0.01 vol% nanowire-Ppy	1 170 000	667 000	0.75		
Ge-0.1 vol% nanowire-Ppy	1 970 000	965 000	1.04		
Ge-0.5 vol% nanowire-Ppy	447 100	234010	0.88		
Ge-1 vol% nanowire-Ppy	406 180	203 401	0.99		



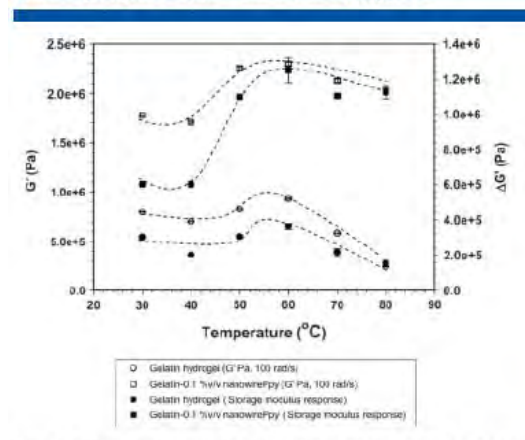


Figure 7. Effect of concentration of particles on the storage modulus (G) and the storage modulus response ( $\Delta G$ ) at various temperatures (sample diameter 30 mm, gel thickness 1.405 mm, 0.15% strain, electric field strength 800 V mm<sup>-1</sup>, frequency 100 rad s<sup>-1</sup>).

increment drastically increases with temperature consistent with classical network theory (40–60 °C). From the results shown, the electromechanical responses of nanowire-Ppy/gelatin hydrogel are mainly improved in terms of storage modulus response ( $\Delta G'$ ) via Ppy polarization. With the presence of nanowire-Ppy,  $G'_{800V/mm}$  and  $\Delta G'$  at any temperature are higher than those of the pure gelatin hydrogel since the nanowire-Ppy acts as a filler and creates a wire-to-wire dipole interaction under an electric field.

#### Deflection of nanowire-Ppy/gelatin hydrogels

The deflection of the pure gelatin and nanowire-Ppy/gelatin hydrogels was studied by vertically suspending the films in a silicone oil bath; a DC electric field was applied horizontally between two parallel flat copper electrodes, as shown in Fig. 8. The amount of deflection at a specified electric field strength is defined by the geometrical parameters – d, l and  $\theta$  – which are illustrated in Fig. 8. The tip displacement of the film was recorded by a digital video recorder (Sony, Handicam HR1). Figures 9(a)-9(c) show the bending of the pure gelatin and the nanowire-Ppy/gelatin hydrogels immersed in the silicone oil with an electric field strength of 600 V mm<sup>-1</sup>. Upon applying an electric field, the free lower end of the film deflects towards the anode side by an amount, depending on the field strength, that results from the effect of the non-symmetric charges. The pure gelatin hydrogel indicates an attractive interaction between the anode and the polarized carbonyl group, in which the gelatin structure possesses negative charge. The deflection distances of the pure gelatin and the nanowire-Ppy/gelatin hydrogels under the electric field are shown in Figs 10(a) and 10(b). The pure gelatin hydrogel shows greater deflection values than the nanowire-Ppy/gelatin hydrogels. The hydrogels start to deflect at lower critical electric field strengths: 25 V mm-1, 300 V mm-1 and 400 V mm-1 for the pure gelatin hydrogel, the nanowire-Ppy(0.1 vol%)/gelatin and the nanowire-Ppy(1 vol%)/gelatin hydrogel, respectively. Moreover, the nanowire-Ppy/gelatin hydrogels show a lesser deflection response under an applied electric field than the pure gelatin hydrogel due to its initial higher rigidity, or its higher  $G'_o$  value.

Figures 10(a) and 10(b) show the deflection distances and the dielectrophoresis forces of the pure gelatin and the

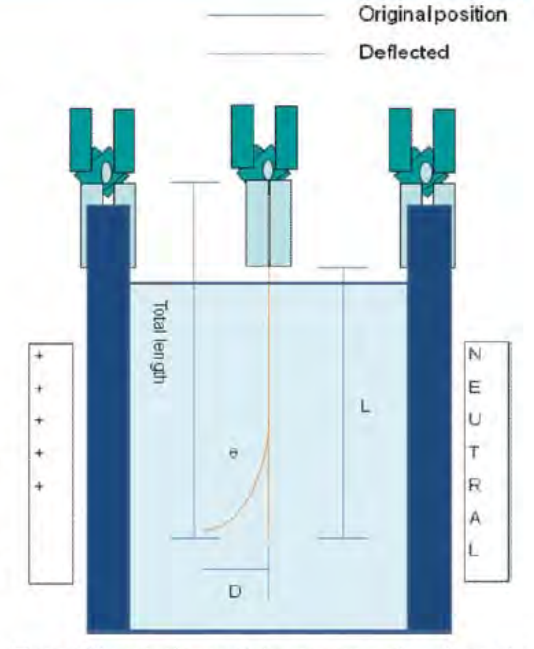


Figure 8. Schematic diagram of the apparatus used to observe the dielectrophoretics of the hydrogel samples.

nanowire-Ppy/gelatin hydrogels under an electric field. The deflection distances and dielectrophoresis forces of the pure gelatin and the nanowire-Ppy/gelatin hydrogels appear to increase stepwise with increasing electric field strength. The dielectrophoresis force at  $E = 600 \,\mathrm{V} \,\mathrm{mm}^{-1}$  for the pure gelatin hydrogel, the nanowire-Ppy(0.1 vol%)/gelatin hydrogel and the nanowire-Ppy(1.0 vol%)/gelatin hydrogel is 7.05, 6.60 and 1.60 mN, respectively. Surprisingly, the resultant dielectrophoresis forces of the nanowire-Ppy/gelatin hydrogels under the applied electric field are smaller than those of the pure gelatin hydrogel. It appears that the induced dipole moments generated by nanowire-Ppy counteract those of the pure gelatin. Under an applied electric field, pure gelatin hydrogel can polarize and generate non-symmetric negative charges. On the other hand, the nanowire-Ppy has strong positive charges attached on the main chains. Apparently, the presence of positive charge diminishes the non-symmetric negative charges generated within the gelatin matrix. Therefore, the bending and the dielectrophoresis forces of the nanowire-Ppy/gelatin hydrogels under an electric field are less.

In previous work, Thongsak  $et al.^{33}$  reported the dielectrophoresis force of styrene–isoprene–styrene triblock copolymer (SIS D1114P): the maximum deflection distance and the dielectrophoresis force at  $E=600\,\mathrm{V}$  mm $^{-1}$  were 2.86 mm and 36.4 µN, respectively. Dai  $et al.^{34}$  studied the bending force under an applied electric field of an ionic network membrane based on blends of water-soluble poly(vinyl alcohol) and highly ionic conductive poly(2-acrylamido-2-methyl-1-propane)sulfonic acid. The bending force of the blend was equal to 4.9 mN at  $E=40\,\mathrm{V}$  mm $^{-1}$ . Kunanuruksapong and Sirivat $^{35}$  studied the electromechanical response of an acrylic elastomer (AR70). The maximum deflection



Figure 9. Deflection of the hydrogels at E=0 and  $600\,\mathrm{V}\,\mathrm{mm}^{-1}$ ; (a) pure gelatin hydrogel; (b) 0.1 vol% nanowire-Ppy/gelatin hydrogel; (c) 1 vol% nanowire-Ppy/gelatin hydrogel. Note that the polarity of the electrode on the left-hand side is positive.

distance and dielectrophoresis force at an electrical strength of  $225 \,\mathrm{V}\,\mathrm{mm}^{-1}$  was  $12.41 \,\mathrm{mm}$  and  $0.367 \,\mathrm{mN}$ , respectively. For the pure gelatin and nanowire-Ppy/gelatin hydrogels studied in this work, the maximum deflection distance and dielectrophoretic force were obtained for the pure gelatin hydrogel at  $E = 600 \,\mathrm{V}\,\mathrm{mm}^{-1}$ . They were  $14.84 \,\mathrm{mm}\,\mathrm{and}\,7.055 \,\mathrm{mN}$ , respectively.

#### CONCLUSIONS

In this study, the electromechanical properties, the storage modulus response under oscillatory shear mode and the cantilever bending, of pure gelatin and nanowire-Ppy/gelatin hydrogels were investigated as functions of electric field strength and operating temperature. In the pure gelatin hydrogel and nanowire-Ppy/gelatin hydrogels with 0.01, 0.1, 0.5 and 1 vol%, the storage modulus (G'), the storage modulus response ( $\Delta G'$ ) and the storage modulus sensitivity ( $\Delta G'/G_0$ ) increase monotonically with increasing electric field strength up to 800 V mm $^{-1}$ . The maximum storage modulus sensitivity was 104% for the nanowire-Ppy(0.1 vol%)/gelatin hydrogel at an electric field strength of 800 V mm $^{-1}$ . The mechanism for the storage modulus response is the interaction

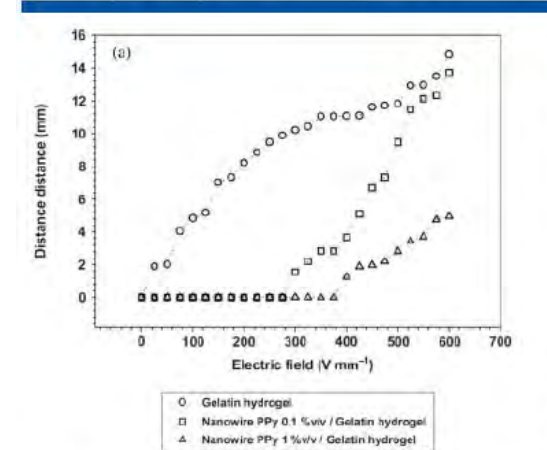
between electrically polarized nanowire-Ppy which induces an electrostatic interaction and the effect of particles acting as fillers. In the presence of nanowire-Ppy, G' and  $\Delta G'$  at any temperature investigated are higher than those of the pure gelatin hydrogel since the nanowire-Ppy acts as a filler and creates a wire-to-wire dipole interaction in an electric field. For the deflection measurement, the deflection distances and the dielectrophoresis forces of the pure gelatin and nanowire-Ppy/gelatin hydrogels increase monotonically with increasing electric field strength. In the case of the nanowire-Ppy(1 vol%)/gelatin hydrogel it possesses the lowest deflection response relative to the others due to its initially higher rigidity or its higher  $G'_o$  value. However, the nanowire-Ppy(0.1 vol%)/gelatin hydrogel is shown overall here to be more electroactive than the pure gelatin hydrogel.

#### **ACKNOWLEDGEMENTS**

The authors would like to acknowledge financial support from the Conductive and Electroactive Polymers Research Unit of Chulalongkorn University; the Thailand Research Fund (TRF-MRG); the Royal Thai Government; Nanotec; the National Conter

The mechanism fo





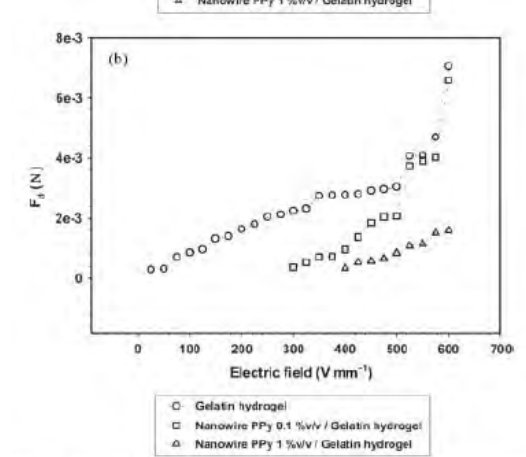


Figure 10. (a) Deflection distances of the gelatin hydrogel, the 0.1 vol% nanowire-Ppy/gelatin hydrogel, and the 1 vol% nanowire-Ppy/gelatin hydrogel at various electric field strengths. (b) Dielectrophoretic force calculated through linear deflection theory.

of Excellence for Petroleum, Petrochemicals, and Advanced Materials; and the Petroleum and Petrochemical College (PPC), Chulalongkorn University. T. Tungkavet acknowledges a Doctoral Scholarship received from the Thailand Graduate Institute of Science and Technology (TGIST) (TG-33-09-53-003D).

#### REFERENCES

- Shahinpoor M, Bar-Cohen Y, Simpson JO and Smith J, Smart Mater Struct 7:R15 – R30 (1998). Calvert P and Liu Z, Acta Mater 46:2565 – 2571 (1998).
- MacDiarmid AG, Chiang JC, Halpern M, Huang WS, Mu SL, Somasiri NL, et al, Mol Cryst Liq Cryst 121:173 180 (1985).
- Zhang QM, Bharti V and Zhao X, Science 280:2101 2104 (1998). Perline RE, Kornbluh RD and Joseph JP, Sensor Actuat Phys A 64:77 85
- (1998).
- Kim J and Seo YB, Smart Mater Struct 11:355-360 (2002).
- Bar-Cohen Y, Electroactive Polymer (EAP) Actuators as Artificial Muscles: Reality, Potential, and Challenges, SPIE, Washington (2001).
- Koyama K, Minagawa K, Watanabe T, Kumakura Y and Takimoto J, J Non-Newtonian Fluid Mech 58:195–206 (1995).
- Yang XJ, Zheng PJ, Cui ZD, Zhao NQ, Wang YF and Yao KD, Polym Int 44:448–452 (1997).
- 44:448-49-2 (1997).
   Marois Y, Chakfe N, Deng X, Marois M, How T, King M, et al, Biomaterials 16:1131-1139 (1995).
   Ross-Murphy SB, Polymer 33:2622-2627 (1992).
   Haider S, Park SY, Saeed K and Farmer BL, Sensor Actuat B: Chem

- Haider S, Park SY, Saeed K and Farmer BL, Sensor Actuat B: Chem 124:517–528 (2007).
   Puvanatvattana T, Chotpattananont D, Hiamtup P, Niamlang S, Sirivat A and Jamieson AM. React Funct Polym 66:1575–1588 (2006).
   Skotheim TA, Elsenbaumer RL and Reynolds JR, Handbook of Conducting Polymers, Marcel Dekker, New York, p. 483 (1998).
   Yang Y and Wan M, J Mater Chem 11:2022–2027 (2001).
   Athawal AA, Kater DP, Phasea SM, and Marcel St. Parkers.
- 16 Athawale AA, Katre PP, Bhagwat SV and Dhamane AH, J Appl Polym Sci 108:2872-2875 (2008).
- 17 Waghuley SA, Yenorkar SM, Yawale SS and Yawale SP, Sensor Actuat B: Chem 128:366-373 (2008).
- Duchet J. Legras R and Demousteir-Champagne S, Synthetic Met 98:113–122 (1998).

- He C, Yang C and Li Y, Synthetic Met 139:539–545 (2003). Sato T, Watanabe H and Osaki K, Macromolecules 29:6231–6239 (1996). Timoshenko SP and Goodier JN, Theory of Elasticity, McGraw-Hill. Auckland (1970).
- Prissanaroon W, Ruangchuay L, Sirivat A and Schwank J, Synthetic Met 114:65-72 (2000). Diaz F and Hall B, IBM J Res Dev 27:342-347 (1983)
- Street GB, Lindsey SE, Nazzal Al and Wynne KJ, Mol Cryst Liq Cryst 118:137–148 (1985).
   Shen Y and Wan M, Synthetic Met 96:127–132 (1998).
   Kwon WJ, Suh DK, Chin BD and Yu JW, JAppl Polym Sci 110:1324–1329.
- (2008)
- 27 Martin CR, Science 266:1961-1966 (1994).
- Shiga T, Deformation and Viscoelastic Behavior of Polymer Gels in Electric Fields, Advances in Polymer Science, Springer-Verlag, Berlin, p. 134 (1997)
- Liu B and Shaw TM, J Rheol 45:641 657 (2001).
   Kunanuruksapong R and Sirivat A, Mat Sci Eng A 454 455:453 460 (2007).
- Bigi A, Panzavolta S and Rubini K, Biomaterials 25:5675-5680 (2004).
- Fraga AN and Williams RJJ, Polymer 26:113-118 (1985).
- Thongsak K, Kunanuruksapong R, Sirivat A and Lerdwijitjarud W, Mat Sci Eng A 527:2504–2509 (2010).
- Dai CA, Kao A, Chang C, Tsai W, Chen W, Liu W, et al, Sensor Actuat A-Phy 155:152–162 (2009).
- 35 Kunanuruksapong R and Sirivat A, Curr Appl Phys 11:393-401 (2011).

[2] Thawatchai Tungkavet, Datchanee Pattavarakorn and Anuvat Sirivat, Bio-compatible Gelatins (Ala-Gly-Pro-Arg-Gly-Glu-4Hyp-Gly-Pro-) and Electromechanical properties: effects of temperature and electric field", Journal of Polymer research (2012), 19, 9759-9767.

J Polym Res (2012) 19:9759 DOI 10.1007/s10965-011-9759-3

ORIGINAL PAPER

# Bio-compatible gelatins (Ala-Gly-Pro-Arg-Gly-Glu-4Hyp-Gly-Pro-) and electromechanical properties: effects of temperature and electric field

Thawatchai Tungkavet · Datchanee Pattavarakorn · Anuvat Sirivat

Received: 6 February 2011 / Accepted: 7 September 2011 / Published online: 23 December 2011 © Springer Science+Business Media B.V. 2011

Abstract Gelatin (Ala-Gly-Pro-Arg-Gly-Glu-4Hyp-Gly-Pro-) is a protein produced by the partial hydrolysis of a collagen extracted from bones, connective tissues, organs, and some intestines of animals. In this work, gelatin films were prepared by the film casting method in an aqueous solvent. The electromechanical properties, thermal properties, and the degree of swelling were investigated as a function of gelatin crosslinking ratio or the gel strength, temperature, frequency, and electric field strength. The high, medium, low, and the 3% crosslinked high-gel-strength gelatin films possess the storage modulus sensitivity values of 2.30, 2.16, 1.26, and 0.49, respectively; these values are much greater than those of other electroactive materials, suggesting the gelatins studied as a potential artificial muscle or actuator.

**Keywords** Gelatin · Gel strength · Electromechanical properties · Actuator · Artificial muscle

#### Introduction

The exchange of electrical energy and mechanical energy has been of scientific and technological interest for many

T. Tungkavet · A. Sirivat (

Conductive and Electroactive Polymers Research Unit. The

Petroleum and Petrochemical College, Chulalongkorn University, Soi Chula 12, Phyathai Rd., Bangkok 10330, Thailand e-mail: anuvat.s@chula.ac.th URL: www.cepru.research.ac.th

D. Pattavarakorn Department of Industrial Chemistry, Faculty of Science, Chiang Mai University, Chiangmai 50200, Thailand

structural proteins found in the animal body: skin, tendons, cartilage, and bone [2]. Gelatin contains a large number of glycine (almost 1 in 3 residues, arranged every third residue), proline and 4-hydroxyproline residues. A typical structure is: Ala-Gly-Pro-Arg-Gly-Glu-4Hyp-Gly-Pro; it is unique in that it contains 14% hydroxyproline, 16% proline and 26% glycine. The only other animal product containing hydroxyproline is the elastin and then at a very much lower concentration, so hydroxyproline is used to determine the collagen or gelatin content of foods. It is a good film and particle forming material [3]. Due to a wealth of merits, such as biological origin, non-immunogenicity, biodegradability, biocompatibility, and commercial availability at relatively low cost, gelatin has been widely used in the pharmaceutical and medical fields as sealants for vascular prostheses, as carriers for drug delivery, as wound dressings, and as artificial muscle [4]. Nevertheless, gelatin exhibits poor mechan-

ical properties, which limits its possible application as a

biomaterial. The improvement of the mechanical properties

of drawn gelatin has been related to the renaturation level of

the protein, as evaluated through the differential scanning

decades. Electromechanical energy conversion has been used in many applications, such as in muscle/insect-like actuators, robotics, etc. [1]. The development of electroactive materials for artificial muscle or actuators is sought after because of their many advantages. First, electroactive materials resemble natural living tissues more than any other classes of synthetic biomaterials because of their high water content, the soft consistency, and their high activation modes. Second, they are biocompatible, but not biodegradable. Third, their physical and chemical properties vary with composition and can be tailored as desired. Fourth, they can take various shapes and are low-cost material.

Gelatin is a protein biopolymer derived from the partial

hydrolysis of native collagens, which are the most abundant



Page 2 of 9

T. Tungkavet et al.

calorimetry [5]. The most interesting feature of gelatin is that it can be used for the production of practical biocompatible materials [6, 7]. Several physical and chemical methods have been reported for crosslinking collagenous materials. Physical methods include the dehydrothermal treatment and the UV irradiation [8, 9]; however, they are generally less efficient. Many chemicals-such as formaldehyde, glutaraldehyde, carbodiimide, and dextran dialdehyde-have been used to chemically modify the gelatin towards biomedical applications. Among them, glutaraldehyde (GTA) is by far the most widely used, due to its high efficiency in stabilizing the collagenous materials [10]. GTA-based crosslinking of collagenous materials significantly reduces biodegradation, making the materials biocompatible and nonthrombogenic, while preserving biological integrity, strength, and flexibility. GTA is also easily available, inexpensive, and capable of allowing the crosslinking in a relatively short time period.

In our work, we are interested in the development of gelatin as a candidate of an artificial muscle or actuator. The electromechanical properties, the thermal properties, and the degree of swelling were investigated and are reported here as functions of the gelatin strength, the crosslinking ratio, temperature, frequency, and electric field strength.

#### Experimental

#### Materials

Gelatin powder (high, medium, and low gel strengths; 250 g bloom, 180 g bloom, and 80 g bloom, respectively) (AR grade, Fluka). The Bloom value is proportional to the storage modulus of the gelatin and it decreases with decreasing Mn [11]., and glutaraldehyde (50% GTA solution) (AR grade, Sigma-Aldrich) were used as the starting materials for fabricating gelatin films. Table 1 shows data on characterization of our samples.

Preparation of gelatin films

Glutaraldehyde–gelatin crosslinked films (GTA–Ge) were prepared by adding an appropriate volume of GTA solution into a 10 vol% gelatin solution with GTA concentrations varying from 0.5 to 7 vol%. Non-crosslinked gelatin films (Ge) were prepared from an aqueous gelatin solution (10%, v/v) at 50 °C and under a continuous stirring for 40 min. The GTA-Ge and Ge solutions were poured into plastic petri dishes (10 cm in diameter). Crosslinked films were obtained after allowing water evaporating at a room temperature for a period of 4 days. Figure 1 shows a schematic of the two proposed structures for gelatin—GA complexes and Pristine gelatin films (Ge) were prepared in a similar way, but without adding the crosslinking agent.

Characterization and testing of gelatin samples

#### Crosslinking density determination

In order to estimate the network crosslinking density, the number-average molecular weight of the chain segments between two crosslinking points,  $M_c$ , was calculated from equilibrium water uptake experiments performed at 20 °C, according to the Flory-Rehner equation [12]:

$$Mc = \frac{\rho V 1 \left( \phi g^{1/3} - 2\phi g / f \right)}{\chi \phi g^2 + \ln(1 - \phi g) + \phi g},$$
(1)

where  $\rho$  is the density of the dry gelatin determined by picnometry,  $V_1$  is the molar volume of the solvent,  $\chi$  is the polymer–solvent interaction parameter taken from the literature [12] ( $\chi$ =0.49±0.05), and  $\varphi_g$  is the volume fraction of the swollen gelatin, which is estimated from the following relation:

$$\phi g = \frac{W_0 \rho w}{W \rho g - W_0 (\rho - \rho w)}, \qquad (2)$$

Table 1 Data on characterization of gelatin

Sample	Non-crosslinked high gel strength gelatin	Non-crosslinked medium gel strength gelatin	Non-crosslinked low gel strength gelatin	
Gel strength	250 g bloom*	180 g bloom*	80 g bloom*	
pH	7.7	6.7	7.0	
Calcium(%)	≤0.2	≤0.2	≤0.2	
Chloride(%)	≤0.2	≤0.2	≤0.2	
% Moisture	≤20	≤20	≤20	
Molecular weight	75,537	57,909	41,363	

<sup>\*</sup>Bloom is the weight in grams required to push a piston of a strictly defined shape 4 mm into a gelatin gel matured for 18 h at 10 C

<sup>\*</sup>Molecular weight as measured by Ubblohde viscometer (K=1.66x10<sup>-5</sup>, a=0.855)



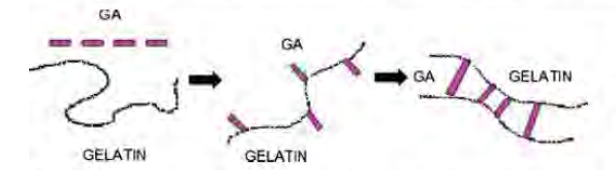


Fig. 1 Schematic of the two proposed structures for gelatin—GA complexes

where  $W_0$  is the initial weight of the sample, W is the weight of the swollen sample,  $\rho_{\rm w}$  is the density of the water at room temperature, and  $\rho$  is the density of the dry and the uncrosslinked gelatin film.

#### Thermogravimetric analysis (TGA)

A thermal gravimetric analyzer (DuPont, model TGA 2950) was used to determine the amount of moisture content and the decomposition temperatures with a temperature scan from 30 to 600 °C with a heating rate of 5 °C/min, for the crosslinked films with% volumes of glutaraldehyde of 0.5,1, 3, 5, and 7, and the non-crosslinked gelatin films. The samples weighed from 5 to 10 mg were loaded into platinum pans and then heated under a nitrogen gas flow.

#### DSC analysis of gelatin films

The thermal properties of the pure gelatin at various gel strength were studied by DSC, (Instruments DSC METTLER 822), using 5 mg of various gel strength gelatin. All measurements were performed under nitrogen atmosphere at a heating rate of 5 °C/min.

#### Electromechanical and thermal properties

The electrorheological properties of the crosslinked and uncrosslinked gelatins were investigated in terms of frequency, temperature, and electric field strength. A melt rheometer (Rheometric Scientific, ARES) was fitted with a parallel-plate fixture (diameter of 25 mm). A DC voltage was applied with a DC power supply (Instek, GFG8216A), which could deliver electric field strengths up to 1 kV/mm. A digital multimeter was used to monitor the voltage input. In these experiments, an oscillatory shear strain was applied and the dynamic moduli (G' and G") were measured as functions of frequency and electric field strength. Strain sweep tests were first carried out to determine the suitable strains to measure G' and G" in the linear viscoelastic regime. The appropriate strain was determined to be 0.2% for the gelatin film samples. For the 3% crosslinked high gel

strength gelatin film sample, a strain of 0.14% was used. Frequency sweep tests were carried out to measure the G' and G" of each sample as a function of frequency. The deformation frequency was varied from 0.1 to 100 rad/s. Prior to each measurement, the non-crosslinked gelatin and the 3% high-gel-strength gelatin film samples were presheared at a low frequency (0.04 rad/s) under an electric field for 15 min to ensure the formation of equilibrium polarization before the G' and G" measurements. The experiments were carried out at a temperature of 27 °C and repeated at least two or three times. The effect of temperature was studied at various temperatures between 27 and 107 °C for the non-crosslinked gelatin film sample. The temporal response experiments were carried out at 1 kV/mm for the non-crosslinked gelatin and the 3% crosslinking high-gel-strength gelatin film samples. Deflection of Gelatin films was carried out under various applied electric strengths. For each film, one end of the sample was fixed with a grip vertically in a transparent chamber containing two parallel electrodes. The input DC field was provided by a DC power supply (Gold Sun 3000, GPS 3003D) and a high voltage power supply (Gamma High Voltage, UC5-30P), which delivered various electric field strengths, from 25 to 600 V/mm. A digital video recorder (Sony handicam, HR1) was used to record the displacement of the films. The tip displacement was measured and calculated from a Scion Image (Beta 4.0.3) program.

We can calculate the static force balance, the deflecting force or the dielectrophoretic force  $(F_d)$  on the samples equals to the sum of the resisting elastic force  $(F_e)$  and the weight along the bending direction, where the film deflection distance at equilibrium is d. The dielectrophoretic force (N) is determined from the static force balance equation as:

$$F_d = F_e + mg\sin\theta,\tag{3}$$

where m is the sample's mass (kg), g is the gravity (9.8 m/s<sup>2</sup>),  $\theta$  is the deflection angle, and  $F_e$  is the resisting elastic force (N). In our experiment, the film deflections with increasing electric field are linear. The linear deflection theory of one free-end film is, therefore, used where the elastic force can be calculated by the following equation [30–32]:

$$F_e = \frac{dEI}{B}, \qquad (4)$$

where E is the elastic modulus which is equal to 2 G'(1+v) in which G' is the shear modulus and  $\nu$  is the Poisson's ratio, which is equal to 1/2 for an incompressible material, I is the moment of inertia, equal to  $t^3w/12$ , where t is the sample thickness, w is the sample width, d is the deflection distance, and I is the sample length.



Page 4 of 9

T. Tungkavet et al.

#### Results and discussion

Determination of degree of swelling, weight loss of gelatin film, and molecular weight between crosslinks and Spectra of Gelatin

Crosslinked and un-crosslinked gelatin films were prepared under the same conditions, and they were kept in a desiccator at room temperature (27 °C) for a period of 2 days before testing to minimize any property changes during the experiments. Glutaraldehyde (GTA) is a fast-acting crosslinker for collageneous materials. The reaction of gelatin with different amounts of GTA was carried out at 50 °C in basic conditions [13]. All crosslinked films were stiffer than pure gelatin films, and they changed thier color to yellowish. Figure 2 shows a pure gelatin film and a 3% crosslinked gelatin films. The 3% crosslinked film becomes more yellowish and slightly shrin. The color change is due to the formation of the aldimine linkages (CH = N) between the free amine groups of the protein and glutaraldehyde [14].

The FTIR spectra of the uncrosslink gelatins show peaks at 1,630 cm<sup>-1</sup>due to the C = O streching, 1,550 cm<sup>-1</sup> due to the N-H bending, and 2,922 cm<sup>-1</sup> due to the C-H stretching. In the spectrum of the 3%v/v crosslinked gelatin film, an additional peak appears at 1,641 cm<sup>-1</sup>. This peak is a characteristic of the aldimine stretching vibration which reveals the crosslinking of gelatin with glutaraldehyde [14]. For the uncrosslinked high gel strength gelatin, the uncrosslinked low gel strength gelatin, and the uncrosslinked low gel strength gelatin, they are of the same of molecular structure

The GTA crosslinking induces a significant reduction in swelling. Swelling measurements at longer times were hindered by the solubility of the film, which began to dissolve in the solution. The calculated average molecular weight between two crosslinking points, Mc, as a function of



Fig. 2 The image of comparison appearance gelatin films



GTA concentration decreases drastically with GTA content, due to the formation of a denser network. Percentages of the crosslinking agent higher than 3 v/v.% (Molecular weight between crosslinked=1,920±296 g/mol) did not induce further changes as no further reaction occurred. Similar results were reported by Fraga and Williams [15], as caused by the termination of the reaction due to the vitrification in thermosetting systems. In addition, gelatin films with a percentage of crosslinking agent higher than 3 wt% do not possess any noticeable differences in the degree of swelling and the percentage of weight loss.

The thermal properties were obtained from the thermogravimetric analysis and the differential thermal analysis (TGA-DTA). The TGA data provide the thermal stability in the terms of onset degradation temperature and% weight residue of the gelatin samples of different Bloom indices and at various percentages of crosslinking ratios between 0%v/v (non-crosslinked gelatin) to 7%v/v (Crosslined gelatin). There are two transitions for the gelatin, namely: the first transition (45 to 100 °C), can be refered to the loss of water; and the second transition (240 to 360 °C), can be refered to the degradation of the gelatin backbone. The TGA thermograms of the non-crosslinked gelatin and the crosslinked gelatin show that the decomposition temperatures are not significantly different; the 7%v/v GTA-Ge has highest percentage of weight residue.

DSC, a widely used thermoanalytical technique, was assess some of the physicochemical properties, such as endothermic or exothermic processes, characteristic of the Gelatin films at various gel strength. It shows typical thermograms recorded from the uncrosslinked gelatin films (High gel strength, Medium gel strength, Low gel strength, and 3%v/v Crosslinked high gel strength gelatin) which exhibit endothermic peak which can be refered to the melting temperatures [16]. For 3%v/v Crosslinking high gel strength gelatin, the melting temperature is higher than those of the uncrosslinked gelatin films so crosslinking can increases the thermal stability of gelatin films, as shown by the shift of the melting temperature to higher values [16]. The melting temperatures (Tm) of the main endothermic transition of uncrosslinked high gel strength gelatin, uncrosslinked medium gel strength gelatin, uncrosslinked low gel strength gelatin, and 3%v/v crosslinked high gel strength gelatin films were at 85.33, 81.41, 79.08, and 87.58C respectively.

Time dependence of the electrorheological response

We first show the temporal responses of the high, medium, low, and 3% crosslinked high-gel-strength gelatin films by alternately switching on and off an electric field strength of E=1,000 V/mm. The temporal characteristics of each sample were recorded in the linear viscoelastic regime at a strain of 0.14% at frequency of 100 rad/s. Figure 3 shows the

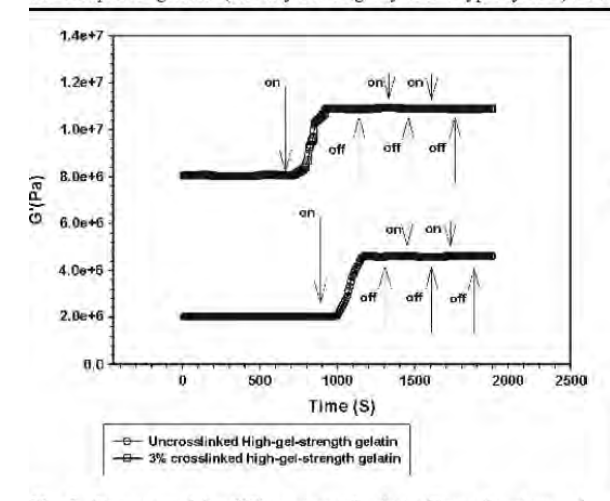


Fig. 3 Storage modulus (G') vs time of gelatin films of various gel strengths (100 rad/s, 1 kv/mm): ○) Uncrosslink High-gel-strength gelatin; and □) 3% crosslinked high-gel-strength gelatin

comparison in storage modulus, G' of the high and 3% crosslinked high-gel-strength gelatin films, during the time sweep test. When the electric field is switched on, the G' values of the high, medium, low, and 3% crosslinked high-gel-strength gelatin films increase from 2 120 000 Pa to 4 570 000 Pa (1.15) in 2,200 s, 835 000 Pa to 1 485 000 (0.79) in 5,000 s, 1 260 000 Pa to 2 080 000 (0.65) in 2,500 s, and 8 060 000 Pa to 10 900 000 Pa (0.35) in 2,000 s, respectively. However, the G' values of the gelatin films do not recover their original values when the electric field is switched off, possibly due to the interaction between the residue dipole moments remaining in the gelatin films [17].

#### Effect of electric field strength

The effect of electric field strength on the rheological properties of the high, medium, low and the 3% crosslinked high-gel-strength gelatin films was investigated in a range of 0 to 1 kV/mm. Figure 4 shows the storage modulus response ( $\Delta G'$ ) of the high, medium, low and the 3% crosslinked high gel strength gelatin films vs. electric field strength at a frequency of 100 rad/s, a strain of 0.14%, and a temperature of 27 °C. The increases in  $\Delta G'$  with electric field strength are nonlinear within the range of 0.1 to 1 kV/mm. The storage modulus response values of these samples at an electric field strength of 1 kV/mm are 4 340 000, 2 820 000, 292 000, and 3 580 000 Pa for the high, medium, low, and the 3% crosslinked high-gel-strength gelatin films, respectively. (The storage modulus sensitivity values of these samples at an electric field strength of 1 kV/mm are tabulated in Table 2; they are 2.30, 2.16, 1.26, and 0.49 for the high, medium, low, and 3% crosslinked high-gel-strength gelatin films, respectively.)

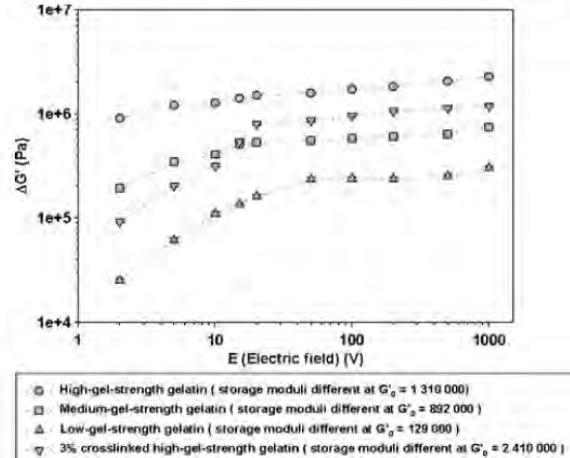


Fig. 4 Storage modulus different vs electric field strength of gelatin films at various gel strengths (100 rad/s, 0.14%strain, 27 °C)

When an electrical field is applied, induced dipole moments within the gelatin structure are generated, leading to intermolecular interactions. These intermolecular interactions induce the loss of free chain movements and thus a higher chain rigidity, as indicated by the higher G' values [18, 19]. The electric field is clearly shown here to enhance the rigidity of the gelatin films. However, the storage modulus of the 3% crosslinked gelatin improves to a lesser degree than those of the uncrosslinked gelatin samples, due to its initially high rigidity in the absence of applied electric field. A higher electric field strength is expected to induce a higher dipole moment and to cause chain segment to pull themselves together in a tighter formation due to the greater electrostatic force, as evidenced by the dramatic increases in G' with electric field strength [20]. Table 3 shows the storage modulus sensitivity characteristics of several electroactive polymers and dielectric elastomers. A sensitivity comparison of these materials can be made between Tables 2 and 3. At an identical electric field strength (1 kV/mm), the styrene-isoprene-styrene triblock (D1114P) exhibits the highest sensitivity in its types, in which the storage modulus sensitivity is 0.122. However, when particles were added to the styrene-isoprene-styrene triblock and the silicone elastomer, the storage modulus sensitivities increased to 0.256 and 0.250, respectively. In our work, the gelatins possess superior responses, as shown in Table 2: the sensitivity values are 2.30, 2.16, 1.26, and 0.49 for the high, medium, low, and 3% crosslinked highgel-strength gelatin films, respectively. These sensitivity values are greater by nearly an order of magnitude than those of pure polymer matrices, triblock copolymers, or elastomers [21, 22], operated at even higher electric field strengths or even with the additions of particles.



Page 6 of 9 T. Tungkavet et al.

Table 2 Comparison of storage modulus sensitivities of the gelatin films of various gel strengths

Material	Electric field (kv/mm)	Frequecy (rad/s)	Temperature °C	Initial storage modulus (G <sub>o</sub> ) Pa	Storage modulus (G') Pa	Storage modulus sensitivity ( $\Delta G'/Go$ ) Pa
Uncrosslinked High-gel-strength gelatin	1,000	100	27	1 310 000	4 340 000	2.30
Uncrosslinked Medium-gel- strength gelatin	1,000	100		892 000	2 820 000	2.16
Uncrosslinked Low-gel-strength gelatin	1,000	100		129 000	292 000	1.26
3% crosslinked high-gel-strength gelatin	1,000	100		2 410 000	3 580 000	0.49

#### Effect of the operating temperature

The rheological properties under an electric field of the uncrosslinked and the crosslinked gelatin films were investigated at operating temperatures of 300 to 380 K. In order to exclude the effect of the gelatin samples,  $G'_{o}$ ,  $G'_{1Kv/mm}$ 

and  $\Delta G'/G'$  are plotted versus temperature as shown in Fig. 5. Here we used one sample each for the  $G'_o$  and  $G'_{1Kv/mm}$  measurements. We can see that the storage moduli decrease linearly with increasing temperature; the deviations may originate from less of chain entanglements in certain temperature ranges.  $G'_{1Kv/mm}$  is higher than that without

Table 3 Comparison of the storage modulus sensitivities of electroactive and dielectric elastomer materials

Materials	Electric field (kv/mm)	Frequecy (rad/s)	Temperature °C	Storage modulus sensitivity (ΔG'/Go) Pa	Ref#
Acrylic elastomer 70	2,000	100	27	0.439	[22]
Acrylic elastomer 71				0.586	
Acrylic elastomer 72				0.148	
Styrene-acrylic copolymers				1.195	
Styrene-isoprene-styrene triblock D1112P				0.746	
Acrylic elastomer 71+PPP 10%(v/v)		1		0.306	
Acrylic elastomer 71+PPP 30%(v/v)				0.971	
Styrene-isoprene-styrene triblock D1114P Styrene-isoprene-styrene triblock D1164P	1,000	1		0.122 0.102	[23]
Styrene-isoprene-styrene triblock D1162P				0.050	
D114P+PDPA 5%(v/v)				0.040	
D114P+PDPA 10%(v/v)				0.256	
D114P+PDPA 30%(v/v)				0.095	
AR71/lead zirconate titanate Pb(Zr0.5Ti0.5)O3 (0.000019%v/v) AR71/lead zirconate titanate Pb(Zr0.5Ti0.5)O3 (0.038%v/v)	2,000	1		0.149 0.587	[24]
poly (dimethyl siloxane) (PDMS) poly (dimethyl siloxane) (PDMS)+PANi 20% (v/v)	2,000	100		0.104 0.25	[25]
poly (dimethyl siloxane) (PDMS)+PANi 2% (v/v)				0.111	
PDMS_5%PEDOT/PSS/EG PDMS_15%PEDOT/PSS/EG	2,000	100		0.077 0.333	[26]
Crosslinked Polyisoprene 3% + Polythiopene 5% (v/v) Crosslinked Polyisoprene 3% + Polythiopene 10% (v/v)	2,000	100	27	0.523 0.33	[27]
Crosslinked Polyisoprene 3% + Polythiopene 30% (v/v)				0.435	
Silicone gel Silicone gel + PMACO 46%	5,000 1,000	60		Not response 0.25	[28, 29]
Silicone gel + PMACO 46%	2,000			0.75	
Silicone gel + PMACO 46%	3,000			2	
Silicone gel + poly(p-phenylenes) 10%	1,000	300		0.333	
Silicone gel + poly(p-phenylenes) 10%	3,000	300		1.133	
Silicone gel + poly(p-phenylenes) 10%	5,000	300		1.666	
Poly(3-hexylthiophene) doped iodine (amorphous)	8.7	-		0.28	



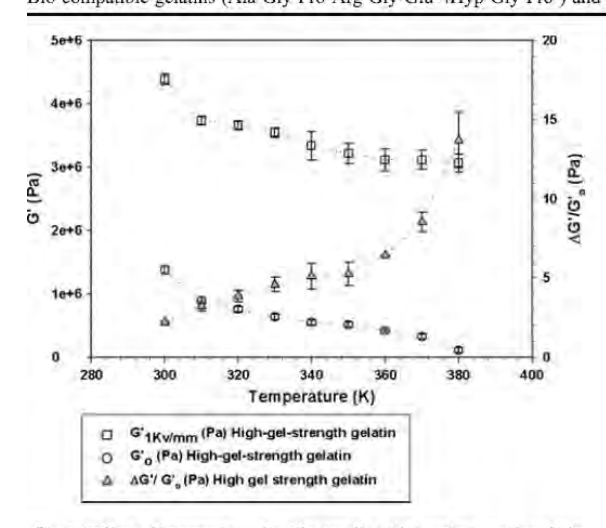


Fig. 5 Effect of temperature for Uncrosslink high-gel-strength gelatin films: Storage modulus (G') at various temperature for one sample at all temperature test (E=0 and 1 Kv/mm, 100 rad/s, 0.14%strain)

electric field at any temperature investigated, as a result of the dipole–dipole interactions created by the electric field within the matrix. The storage modulus sensitivity of the gelatin sample increases significantly as temperature increases; this implies that temperature induce the free chain movement easier without electric field [30].

#### Deflection of gelatin films

The deflection of the gelatin films was studied by vertically suspending the films in a silicon oil bath; and a DC electric field was applied horizontally between two parallel flat copper electrodes, as shown in Fig. 6. The amount of deflection at a specified electric field strength is defined by the geometrical parameters—d, l, and θ—which are illustrated in Fig. 6. The tip displacement of the film was recorded by a digital video recorder (Sony Handicam, HR1). Figure 6 shows the bendings of the high-gel-strength and the lowgel-strength gelatin films immersed in silicone oil under an electric field strength of 600 V/mm. Upon applying an electric field, the free lower end of the film deflects towards the cathode side by an amount dependent on the field strength, indicating an attractive interaction between the cathode and the polarlized amine group, in which the gelatin structure possesses negative charges. (The deflection distance of the gelatin films under electric field is shown in Fig. 7.) The low-gel-strength gelatin film shows a greater deflection value than the high-gel-strength gelatin. The films start to deflect at their critical electric field strengths (600 V/mm). Moreover, the high-gel-strength gelatin film has a lesser deflection response under the applied electric field than the low-gel-strength film due to its initially higher rigidity, or its higher G' value.

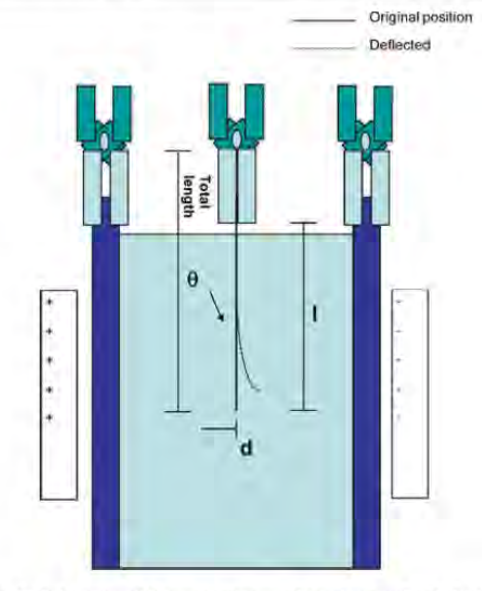


Fig. 6 Schematic of the apparatus used to observe the dielectrophoretics of the gelatin films

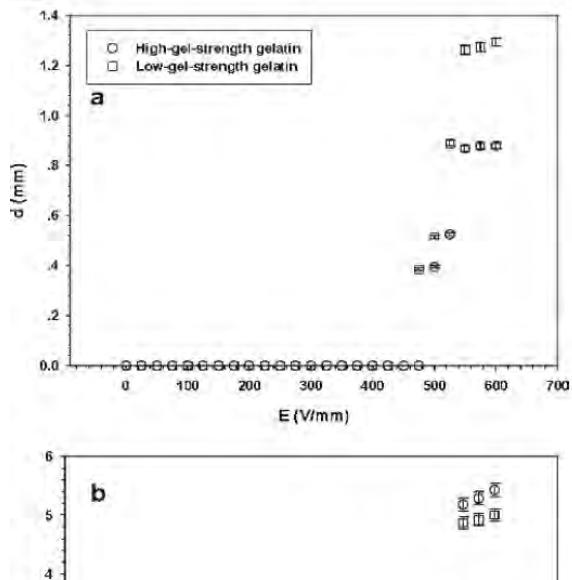
Figure 8 shows the dielectrophoretic force of the gelatin films under electric field. The dielectrophoretic forces of the low-gel-strength gelatin and the high-gel-strength gelatin films appear to increase monotonically with increasing electric field strength. (Table 4 shows the deflection responses achieved under an applied electric field on the gelatin films in terms of the deflection distance (d), the deflection angle (θ), the resisting elastic force (F<sub>e</sub>), and the dielectrophoretic force (F<sub>d</sub>). The resisting elastic force of the low-gel-strength gelatin film under an applied electric field is less than that of the high-gel-strength gelatin film. However, the low-gelstrength gelatin film exhibits a greater response in the bending mode than the others, suggesting its greater flexibility. In previous work, Thongsek et al., [23] reported the dielectrophoresis force of Styrene-Isoprene-Styrene Triblock Copolymer (SIS D1114P), the maximum deflection distance and dielectrophoresis force at E=600 V/mm is 2.86 mm and 36.4  $\mu$ N.



Fig. 7 Deflection of the sample under electric field strength 600 V/mm: a High-gel-strength gelatin; b Low-gel-strength gelatin

Page 8 of 9

70



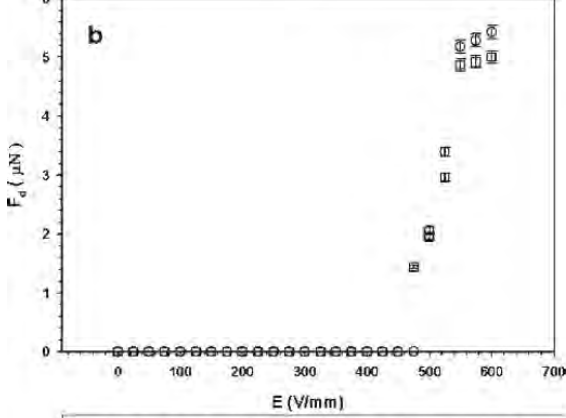


Fig. 8 a Deflection distances of high-gel-strength gelatin and low-gel-strength gelatin at various electric field strengths and b Dielectrophoretic force calculated through the Linear Deflection theory

High-gel-strength gelatin,  $\mathbf{F}_{\mathbf{d}}$  calculated by linear deflection theory

Low-gel-strength gelatin, F<sub>d</sub> calculated by linear deflection theory

respectively. Alici et al., [33] reported that the actuators based on polymer composites between polypyrrole and polyvinylidine fluorine could provide the output force equal to 0.6 mN at E=1 V [26]. Dai et al., [34] studied the bending force under applied electric field of ionic network membrane based on blends of water soluble poly (vinyl alcohol) (PVA) and highly ionic conductive poly 2-acrylamido-2-methyl-1-propanesulfonic acid (PAMPS). The bending force of PVA/PAMPS blend was equal to 4.9 mN at E=40 V/mm [34]. Kunanuruksapong et al., [35] studied electromechanical response of acrylic elastromer (AR70). The maximum deflection distance and dielectrophoresis force at electrical strength (225 V/mm) is 12.41 mm and 0.367 mN, respectively. When comparing with our Gelatin films (low-gel-strength), the maximum deflection distance and dielectrophoresis force at E=600V/mm is 1.28 mm and 4.859 µN, respectively. Our materials

Table 4 Electromechanical responses of the high-gel-strength gelatin and the low-gel-strength gelatin at various electric field strengths

Sa mple	E (V/mm)	d (mm)	1 (mm)	θ (°)	F <sub>e</sub> (μN)	F <sub>d</sub> (μN)
Uncrosslinked High-gel- strength gelatin film	0	0	23.05	0	0	0
	100	0	23.05	0	0	0
	200	0	23.05	0	0	0
	300	0	23.05	0	0	0
	400	0	23.05	0	0	0
	475	0	23.05	0	0	0
	500	0.39	23.05	0.973	0.713	2.054
	525	0.52	23.05	1.305	1.137	2.933
	550	0.86	23.05	2.19	2.118	5.116
	575	0.87	23.05	2.21	2.180	5.217
	600	0.88	23.05	2.26	2.244	5.353
Uncrosslinked	0	0	22.48	0	0	0
Low-gel- strength gelatin film	100	0	22.48	0	0	0
	200	0	22.48	0	0	0
	300	0	22.48	0	0	0
	400	0	22.48	0	0	0
	475	0.38	22.48	0.952	0	0
	500	0.51	22.48	1,293	0.229	1.428
	525	0.88	22.48	2.247	0.317	1.940
	550	1.25	22.48	3.222	0.536	3.351
	575	1.26	22.48	3.25	0.776	4.807
	600	1.28	22.48	3.3	0.792	4.859

give a lower dielectrophoresis force less than those of the polymer composites, the ionic network membrane, and the elastromers. However, the storage modulus sensitivity values of the gelatin are superior to those of the previous work.

#### Conclusions

In our work, the electromechanical properties of gelatin films were investigated as functions of electric field strength and operating temperature in terms the storage moduli under oscillatory shear mode. The storage modulus (G') increases with increasing gel strength, as the applied electric field strength is equal to 1 kV/mm.  $\Delta G'$  and  $\Delta G'/Go$  values of the gelatins increase with increasing temperature. At a temperature above 300 K, the storage moduli decrease linearly with increasing temperature. For the un-crosslinked gelatin films, the storage modulus response and the storage modulus sensitivity are higher than those of the crosslinked gelatin films. The storage modulus sensitivity of gelatin values are greater by nearly an order of magnitude than those of previously studied pure polymer matrices, triblock copolymers, or elastomers which were operated at even higher electric field strengths or even with the additions of



particles. From the deflection measurement, the deflection distances of the low-gel-strength and the high-gel-strength gelatin films increase monotonically with increasing electric field strength. The low-gel-strength gelatin film shows the greatest deflection response.

Acknowledgements The authors would like to acknowledge the financial support to A.S. from the Conductive and Electroactive Polymers Research Unit of Chulalongkorn University, the Thailand Research Fund (TRF-BRG), the Thai Royal Government (Budget of Fiscal Year 2552), and the National Center of Excellence for Petroleum, Petrochemicals, and Advanced Materials.

#### References

- Krause S, Bohon K (2001) Electromechanical response of electrorheological fluids and poly(dimethylsiloxane) networks. Macromolecules 34:7179
- Zhang YZ, Venugopal J, Huang Z-M, Lim CT, Ramakrishna S (2006) Crosslinking of the electrospun gelatin nanofibers. Polymer 47:2911–2917
- Yang XJ, Zheng PJ, Cui ZD, Zhao NQ, Wang YF, Yao KD (1997) Swelling behaviour and elastic properties of gelatin gels. Polym Int 44:448-452
- Marois Y, Chakfe N, Deng X, Marois M, How T, King M (1995) Carbodiimide cross-linked gelatin, a new coating for polyester arterial prostheses. Biomaterials 16:1131–1139
- Bigi A, Cojazzi G, Panzavolta S, Rubini K, Roveri N (2001) Mechanical and thermal properties of gelatin films at different degrees of glutaraldehyde crosslinking. Biomaterial 22:763–768
- Bottoms E, Cater CW, Shuster S (1966) Effect of ultraviolet irradiation on skin collagen. Nature 211:97–8
- Draye JP, Delaey B, Van de Voorde A, Van Den Bulcke A, De Reu B, Schacht E (1998) In vitro and in vivo biocompatibility of dextran dialdehyde cross-linked gelatin hydrogel films. Biomaterials 19:1677–1687
- Schach E, Van Den Bulcke A, Bogdanov B, Draye JP, Delaey B (1998) Gelatin-based hydrogel for wound dressing. Polym Mater Sci Eng 79:222–223
- Fujimori E (1965) Ultraviolet light-induced change in collagen macromolecules. Biopolymers 3:115–9
- Khor E (1997) Methods for the treatment of collagenous tissues for bioprostheses. Biomaterials 18:95–105
- Abrusci C, Martin-Gonzalez A, Amo AD, Corrales T, Catalina F (2004) Biodegradation of type-B gelatin by bacteria isolated from cinematrographic films. A viscometric study. Polym Degrad Stabil 86:283–291
- Flory PJ, Rehner JJ (1943) Statistical mechanics of cross–linked polymer networks II. Swelling. Chem Phys 11:521–526
- Apostolov AA, Boneva D, Vassileva E, Mark JE, Fakirov S (2000) Mechanical properties of native and crosslinked gelatins in a bending deformation. J Appl Polym Sci 76:2041–2048
- Martucci JF, Ruseckaite RA, Vazquez A (2006) Creep of glutaraldehyde-crosslinked gelatin films. Mat Sci Eng A 435– 436:681–686
- Fraga AN, Williams RJJ (1985) Thermal properties of gelatin films. Polymer 26:113–118

- Li M, Guo Y, Wei Y, Macdiamid AG, Lelkes PI (2005) Electrospinning polyaniline-contained gelatin nanofibers for tissue engineering applications. Biomaterials 27:2705

  –2715
- Chotpattananont D, Sirivat A, Jamieson AM (2004) Electrorheological properties of perchloric acid-doped polythiophene suspensions. Colloid Polym Sci 282:357–365
- Perline RE, Kornbluh RD, Joseph JP (1998) Electrostriction of polymer dielectrics with compliant electrodes as a means of actuation. Sensor Actuat Phys A 64:77–85
- Liu B, Shaw TM (2001) Electrorheology of filled silicone elastomers. J Rheol 45:641–657
- Shiga T (1997) Deformation and viscoelastic behavior of polymer gels in electric fields. Advances in polymer science, vol. 134/20. Springer, Berlin
- Pelrin R, Kornbluh R, Joseph J, Heydt R, Pei Q, Chiba S (2000) High-field deformation of elastomeric dielectrics for actuators. Mat Sci Eng C 11:89–100
- Kunanuruksapong R, Sirivat A (2007) Poly(p-phenylene) and acrylic elastomer blendsfor electroactive application. Mat Sci Eng A 454–455:453–460
- Thongsak K, Kunanuruksapong R, Sirivat A, Lerdwijitjarud W (2010) Electroactive styrene-isoprene-styrene triblock copolymer: effects of morphology and electric field. Mat Sci Eng A 527:2504– 2509
- Tangboriboon N, Sirivat A, Kunanuruksapong R, Wongkasemjit S (2009) Electrorheological properties of novel piezoelectric lead zirconate titanate Pb(Zr0.5, Ti0.5)O3-acrylic rubber composites. Mat Sci Eng C 29:1913–1918
- Hiamtup P, Sirivat A, Jamieson AM (2008) Electromechanical response of a soft and flexible actuator based on polyaniline particles embedded in a cross-linked poly(dimethyl siloxane) network. Mat Sci Eng C 28:1044–1051
- Wichiansee W, Sirivat A (2009) Electrorheological properties of poly(dimethylsiloxane) and poly(3,4-ethylenedioxy thiophene)/ poly(stylene sulfonic acid)/ethylene glycol blends. Mat Sci Eng C 29:78–84
- Puvanatvattana T, Chotpattananont D, Hiamtup P, Niamlang S, Sirivat A, Jamieson AM (2006) Electric field induced stress moduli in polythiophene/polyisoprene elastomer blends. React Funct Polym 66:1575–1588
- Shiga T, Okada A, Kurauchi T (1993) Electroviscoelastic effect of polymer blends consisting of silicone elastomer and semiconducting polymer particles. Macromolecules 26:6958–6963
- Shiga T, Okada A, Kurauchi T (1995) Electroviscoelastic effect of doped poly(3-hexylthiophene). J Mater Sci Lett 14:514–515
- Sato T, Watanabe H, Osaki K (1996) Rheological and dielectric behavior of a styrene–isoprene–styrene triblock copolymer in n– Tetradecane. 1. Rubbery–Plastic–Viscous Transition. Macromolecules 29:6231–6239
- Timoshenko SP, Goodier JN (1970) Theory of elasticity, 3rd edn. McGraw-Hill. Auckland
- 32. Gere JM (1972) Mechanics of materials, 3rd edn. Chapman & Hall
- Alici G, Mui B, Cook C (2006) Bending modeling and its experimental verification for conducting polymer actuators dedicated to manipulation applications. Sensor Actuat Phys A 126:396
- 34. Dai CA, Kao A, Chang C, Tsai W, Chen W, Liu W, Shih W, Ma CC (2009) Polymer actuator based on PVA/PAMPS ionic membrane: optimization of ionic transport properties. Sensor Actuat A-Phy 155:152–162
- Kunanuruksapong R, Sirivat A (2010) Effect of dielectric constant and electric field strength on dielectrophoresis force of acrylic elastomers and styrene copolymers. Curr Appl Phys 1-10

# การนำเสนอในที่ประชุมงานวิชาการระดับนานาชาติ

[1] Siripong Thongbor and <u>Datchanee Pattavarakorn</u>, "Electromechanical properties of Electroactive Polythiophene/Elastomer Blend", TIChE International Conference 2011, 10-11 November 2011, Hatyai, Songkhla, THAILAND.

# Electromechanical Properties of Conductive Polythiophene/Poly (dimethyl siloxane) Blend

Siripong Thongbor, Siriluck Chumsaratool, Sujitra Thaithed and Datchanee Pattavarakorn\*

Department of Industrial Chemistry, Faculty of Science, Chiang Mai University, Chiangmai, 50200, Thailand
\*E-mail: cdatchan@chiangmai.ac.th, cdatchanee@hotmail.com

#### Abstract

The conductive polythiophene/poly (dimethyl siloxane) blend (PTh/PDMS blend) was prepared in this research. Polythiophene was synthesized via oxidative polymerization in chloroform at 40 °C and then the PTh/PDMS blend was prepared by mechanical blending of polythiophene particles and PDMS fluid. The specified amount of crosslinking agent; tetraethyl orthosilicate, and catalyst; dibutyltin dilaurate, were added. After that, the electromechanical properties; electrorheological properties and bending response under electric field of the blend were investigated. The effects of polythiophene particle concentration (0-30 %vol) and electric field strength (0-2 kV/mm) were studied. The results showed that the PTh/PDMS blend response well to the electric field. In which, the storage modulus response ( $\Delta$ G') of the blend increased with the increase in polythiophene particle concentration and electric field strength. For the bending response test under electric field, it was found that the increase electric field strength result in the increase of bending angle. Moreover, the PTh/PDMS blend had better response than pure PDMS.

Keywords: Electromechanical, Electrorheology, Conductive polymer, Polythiophene, Polydimethyl siloxane

#### Introduction

Electroactive polymers (EAPs) are polymer materials that change their shape or size in response to electrical stimuli. This class of materials is therefore a good candidate for actuators in the field of medical devices, soft manipulators and biomimetics, since they mimic the behavior of biological muscles [1]. The actuators have been produced for many sizes to a variety of styles application. Various materials have been made as actuator: sharp memory alloys (SMA) and electroactive ceramics [2]. However, these materials have limit in terms of weight and ability to change size or sharp. elastomers are a type of Dielectric electric-field-activated electroactive polymers that are capable of producing large strains, fast efficiency. response. and high (dimethylsiloxane) [PDMS], an elastomer, is a potential candidate material for various actuator applications. It has excellent dielectric Properties and flexibility [3]. Currently, conductive polymer (CPs) is alternative to

produce for actuators instead of a metallic material. The conductive polymers have many advantages over other material such as low cost, relatively simple fabrication, light weight and combine the mechanical properties (flexibility, toughness, elasticity, malleability, etc.) of plastics with high electrical conductivities [4], [5]. Many conductive polymers such as polyacetylene, polythiophene, polypyrole, polyaniline have attracted much attention for their promising applications such as sensors, electrochemical displays, batteries, antistatic coatings, anticorrosive coatings, actuator, artificial muscles, functional membranes and controlled release of ionic drugs, etc. [6].

In this study, we are interested to developing and testing polythiophene/poly (dimethyl siloxane) blend towards actuator applications. The electromechanical properties; electrorheological properties and bending response under electric field are investigated in terms of polythiophene particle concentration and electric field strength.

#### Materials

Thiophene, C<sub>4</sub>H<sub>2</sub>S (AR grade, Fluka) was used as the monomer. Iron (III) chloride anhydrous, FeCl3 (AR grade, Acros organics and Ajax Finechem) was used as the oxidant. Chloroform, CHCl3 (AR grade, labscan Asia) and methanol, CH3OH (AR grade, J.T. baker) were used as recieved. Hydroxyl terminated poly (dimethylsiloxane), OH-[Si(CH<sub>3</sub>)<sub>2</sub>O]<sub>n</sub>-H (viscosity 3,500 cSt. Aldrich) was used as a elastomeric matrix. Tetraethl orthosilicate (TEOS), Si (OC2H5)4 (AR grade, Aldrich) and dibutyltin dilaurate (2EHSn), (CH<sub>2</sub>)<sub>10</sub>OCO]<sub>2</sub>Sn[(CH<sub>2</sub>)<sub>3</sub>CH<sub>3</sub>]<sub>2</sub> (AR grade. Aldrich) were used as a crosslinking agent and a catalyst, respectively.

$$HO = \begin{bmatrix} CH_3 \\ I \\ SI = O \end{bmatrix}_n H$$

Poly(dimethyl siloxane), hydroxy terminated

Fig. 1: Chemical structure of PDMS

#### Experimental

#### Synthesis of polythiophene (PTh)

Polythiophene was synthesized chemical oxidative polymerization [7]. 145 g of FeCl<sub>3</sub> anhydrous was added to 800 ml of chloroform and the mixture was stirred in a 3-necked round bottom flask and heat at 40 °C with silicon oil basin. 24.60 g of thiophene monomer (C4H2S) was added to 100 ml of chloroform in a separatory funnel. thiophene monomer solution was added dropwise to the FeCl3 anhydrous solution with continuous stirring at room temperature for 3 hours. After all the thiophene monomer solution was added, the reaction mixture was continuity stirred at 40 °C for 9.5 hours and the reaction methanol was added to the reaction mixture and stirred for 1.5 hour in order to stop the reaction. Polythiophene particles were filtered using Buchner suction funnel and dried in vacuum oven at 27 °C for 24 hours.

#### Characterization of Polythiophene

Fourier transform infrared spectroscopy (FT-IR, Perkin Elemer, spectrum RX) was used to confirm the chemical structure and identify functional groups of polythiophene. The spectrometer was operated in the transmission mode averaging 32 scans at a resolution of ±4 cm<sup>-1</sup>, covering a wave number range of 400–4000 cm<sup>-1</sup> using a deuterated triglycine sulfate detector. Optical grade KBr was used as a background material. The samples were ground with KBr and pressed to form pellets.

Ultraviolet visible spectroscopy (UV-visible spectroscopy, Hewlett Packard, Hewlett Packard) was used to confirm the synthesis of PTh. UV-vis spectra were investigated with the absorbance in the wavelength and indicated on change of polythiophene chain. The sample was prepared by dissolved in dimethylformamide (DMF, AR grade, labscan Asia). Measurements were set in the absorbance mode in the wavelength range of 190-1000 nm with a tungsten lamp as the light source.

The morphology of the sample was observed with scanning electron microscope (SEM, JEOL, model JSM-S410LV) at an acceleration voltage of 15 kV and a magnification of 3500. Prior to observation, samples were gold sputtered.

The electrical conductivity of polythiophene was measured using two-point probe meter consists of two copper probes. The disc sample (diameter of 30 mm and  $\sim$ 0.5 mm thick), 0.05 g of the polythiophene powder was molded using a hydraulic press under pressure of 5 ton for 4 min. The electrical conductivity under controlled temperature was measured using an electrometer (Keithley, model 2410). The measurements were performed in the linear Ohmic regime where the specific conductivity values are independent of the applied DC voltage. The specific conductivity,  $\sigma$  (S/cm) value of the sample was calculated as follow the relation.

mixture temperature was decreased to room temperature. After that, 800 ml of

$$\sigma = (I/Vt) (1/K) \tag{1}$$

where I is the current change (A), V is the applied voltage (V), t is the sample thickness (cm) and K is the geometric correction factor.

#### Preparation of PTh/PDMS blend

Polythiophene/Poly(dimethylsiloxane) (PTh/PDMS) blend films were prepared according to the method of Haimtup *et.al.* [8]. Polythiphene particles were mixed with HO-PDMS and TEOS at a crosslinking agent to monomer ratio (C/M) of 0.053 (TEOS 0.17 and PDMS 1.40 g), using 2EHSn as the catalyst. The mixture was poured in a mold and allowed to cure under vacuum for 24 hours. The volume fraction of polythiophene particle was varied in the range of 0 to 30 vol. %.

#### Electromechanical properties measurement

The electromechanical properties of conductive PTh/PDMS blend were investigated in the way of electrorheological test and bending response test under the electric field. The effects of polythiophene particle concentration and electric filed strength were studied.

For the electrorheological properties study, PTh/PDMS blend samples with a diameter of 25 mm and a thickness of 1 mm were prepared. The sample was placed between parallel plates (diameter of 25 mm) of a modified melt rheometer (ARES, Rheometric Scientific Inc.) which is attached to a DC power supply. The samples were first checked for viscoelastic linearity by strain sweep tests. Experiments were carried out in the frequency sweep mode ranging from 0.1 to 100 rad/s to investigate the effect of electric field strength on the storage and loss moduli, G' and G". All experiments at each applied field strengths were repeated twice to confirm reproducibility.

Finally, the bending response of the conductive PTh/PDMS blend in an electric field was investigated using the experimental set-up as shown in Fig. 2.

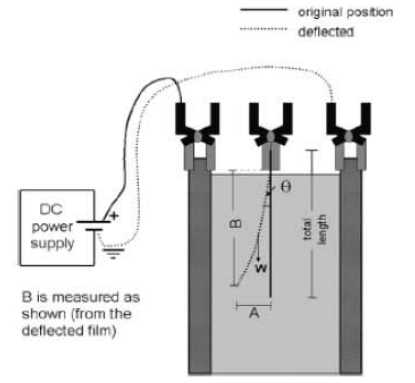


Fig. 2: Schematic diagram of the apparatus used to observe the bending response of the

#### PTh/PDMS blend [8].

The PTh/PDMS films were immersed vertically in a silicon oil (viscosity=100 cSt) bath, with a dc electric field applied horizontally between two parallel flat copper electrodes. DC electric field was applied with various strengths in the range of 0-700 V/mm. The amount of deflection at a specified field strength is defined by the geometrical parameters A, B and  $\theta$ . The bend angle ( $\theta$ ) was calculated from the following equation,

$$\theta = \arctan(A/B) \tag{2}$$

#### Results and Discussion

#### Characterization of polythiophene

The FT-IR spectrum of the synthesized polythiophene is showed in Fig. 3. The spectrum shows characteristic peaks at  $787~\text{cm}^{-1}$ ,  $1219~\text{cm}^{-1}$ ,  $1367~\text{cm}^{-1}$  and  $1736~\text{cm}^{-1}$  corresponding to the C-C bending vibration, C-C stretching vibration of  $\alpha$ -coupled, C-H stretching vibration and C=C stretching vibration of the thiophene ring, respectively.

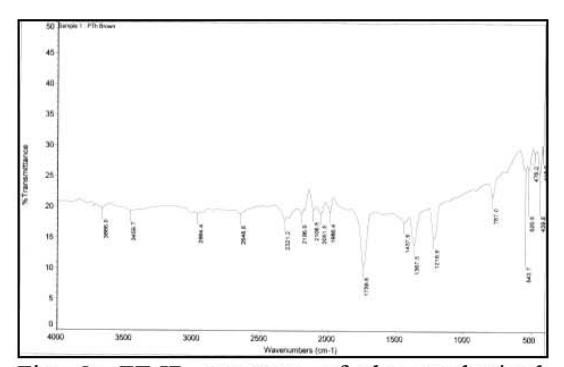


Fig. 3: FT-IR spectrum of the synthesized polythiophene

The UV-Vis absorption spectrum of synthesized polythiophene in DMF solution shows absorption peak at 375 nm and 321 nm, due to the  $n-\pi*$  and  $\pi-\pi*$  transition of the thiophene unit, respectively. Fig. 4 shows the scanning electron microscopy of synthesized polythiophene particles. It can be seen that the shapes of the polythiophene particles and their surfaces are quite irregular. The specific conductivity of synthesized polythiophene was measured using the two-point probe meter. It was found that the specific conductivity of polythiophene is 8.97 x  $10^{-5}$  S/cm.



Fig. 4: The morphology of polythiophene.

# Electrorheological properties of PTh/PDMS blend

The effects of particle concentration and electric field strength on electrorheological properties of the blends were explored. Particle volume fraction investigated was varied from 0 to 30 vol. % and the electric field strength was varied as 0-2 kV/mm. The magnitude of the response is characterized as the difference in storage modulus with the field on  $(G'_E)$  and off  $(G'_{E0})$ ,  $\Delta G' = G'_E - G'_{E0}$ , of the blends.

#### - Effect of particle concentration

In PTh/PDMS blend preparation, only the blends with polythiophene particle concentration of 0-10 vol. % can be molded. While the blends with higher polythiophene volume fraction crack and cannot be removed from mold. Fig. 5 shows the modulus response of the PTh/PDMS blend as a function of polythiophene particle concentration. It was found that the modulus responses of the PTH/PDMS blends with polythiophene volume fraction less than 5 vol. % are lower than pure PDMS. This might because the crosslink in PDMS is obstructed by polythiophene particles. Moreover, the blend with particle fraction of 5 showing a trend of greater electromechanical response; at a field strength of 1 kV/mm. The microscopic attraction between the induced electric dipoles on the polythiophene particles evidently changes in the overall mechanical properties presumably via an electrostriction effect. The blends with a higher volume fraction have stronger electrostatic interactions, since the average distance between particles is smaller, and these forces increase strongly as the interparticle spacing decreases [9]. In addition, the blend with polythiophene particle of 10 vol.% seems to has lower ΔG' than those 5 vol.% blend. This may because higher particle

concentration requires stronger electric field strength for polarization, polythiophene particles are then not completely polarized at 1 kV/mm filed.

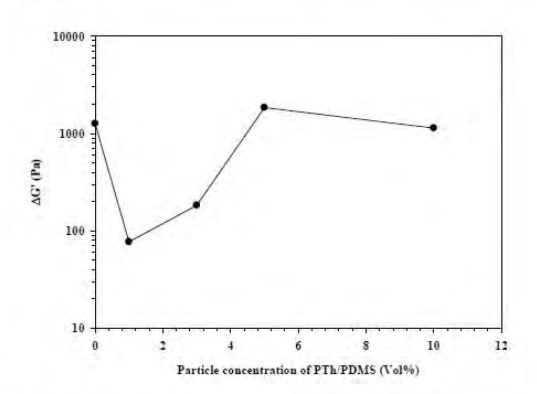


Fig. 5: particle concentration dependence of modulus response  $\Delta G$ ' (at  $\omega=1$  rad/s) of PTh/PDMS blends, measured at E = 1 kV/mm and T = 27 °C.

#### - Effect of electric field strength

Fig. 6 shows the storage modulus response  $(\Delta G')$  vs. electric field strength of pure PDMS PTh/PDMS blend with polythiophene concentrations. It can be seen that the response of each system generally increases with increasing electric field strength. As an electric field is increased, both polythiophene particles and PDMS matrix become more polarize, leading to higher dipole moment and intermolecular interactions. Moreover, the blend with particle fraction 5 vol.% increased marginally with increasing electric field strength due to greater electrostatic interactions as mention above. At the electric field strength of 2 kV/mm, the assertion of result contradiction to the previous research works in which the blend with particle fraction 5 vol.% shows lowest ΔG' response. The rational clarification is still ambiguous unless the characterization in the further experiment is carried out.

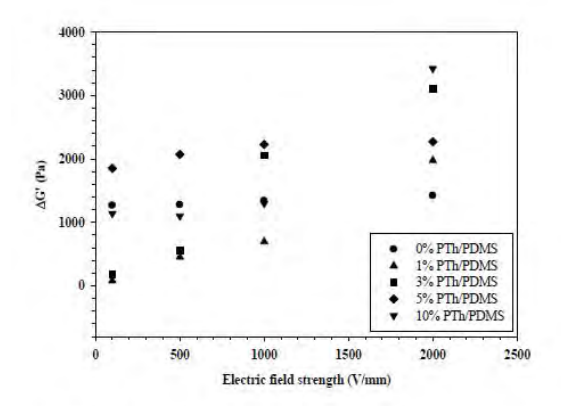


Fig. 6: The storage modulus response ( $\Delta G'$ ) of pure PDMS and PTh/PDMS blends vs. various electric field strengths.

#### Bending response of PTh/PDMS blend

The bending response or deflection of PTh/PDMS blends under electric field was last investigated Fig. 7 shows images of the bending of a PTh/PDMS blend containing 5 vol.% polythiophene particles, immersed in silicone oil at different electric field strengths. The figure shows that on applying the electric field, the free lower end of the blend bends towards the anode by an amount dependent on the field strength. It is indicating an attractive interaction between the applied field and the polarized polythiophene particles in the blend.

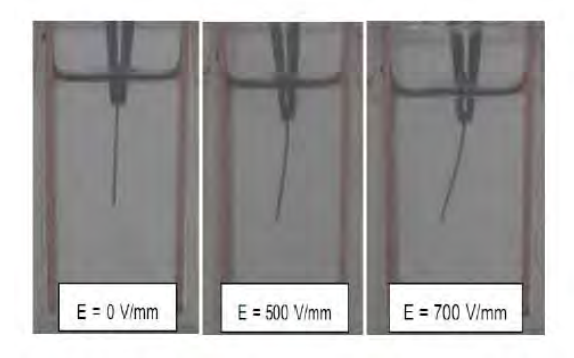


Fig. 7: Bending response of the PTh/PDMS with polythiophene concentration of 5 vol. % at various applied voltages.

The bending angle as a function of polythiophene particle concentration at the field strength of 0.5 kV/mm is shown in Fig. 8. The blends has higher bending angle when the particle concentration increased. The

PTh/PDMS blend with 10 vol. % polythiophene shows maximum bending angle of 12.53°. The increase in bending angle of PTh/PDMS blends can be attributed to the increase of induced polarization which leading to the increase of interactions between polythiophene particles in PDMS matrix and copper electrode.

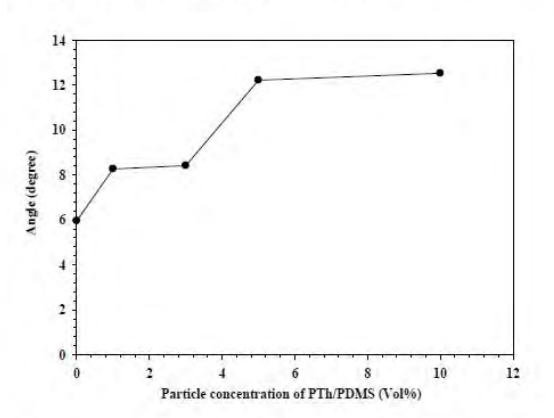


Fig. 8: Bending angle of PTh/PDMS blends with various particle concentrations at electric field strength of 0.5 kV/mm.

Fig. 9 shows the bending angle vs. electric field strength of pure PDMS and 10 vol. % PTh/PDMS blend. The bending response can be observed when applied electric field strength is higher than 0.5 kV/mm for either pure PVDF or 10 vol. % PTh/PDMS sample. The bending angle response appears to increase with increasing of electric field strength, according to greater polarization of polythiophene particles which lead to higher interaction between polythiophene particle and PDMSmatrix.

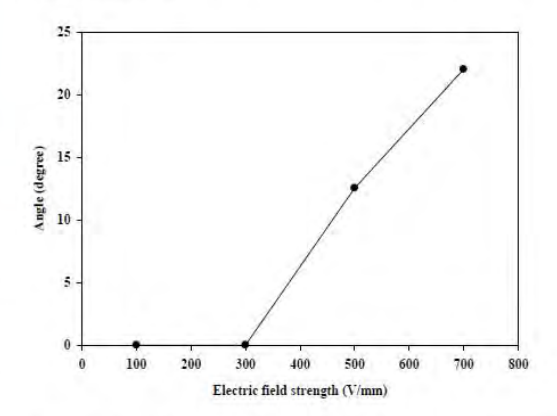


Fig. 9: Bending angle of pure PDMS and 10% PTh/PDMS at various electric field strengths (0, 0.1, 0.3, 0.5 and 0.7 kV/mm).

#### Conclusions

In this study, the electromechanical properties; electrorheological properties and bending response of polythiophene/ poly (dimethyl siloxane), PTh/PDMS blend were investigated by examining the effects of polythiophene particle concentration and electric field strength varying from 0 to 2

polythiophene particle concentration and electric field strength varying from 0 to 2 kV/mm. The storage modulus response ( $\Delta G'$ ) increases with particle concentration and electric field strength due to polythiophene particles and

poly(dimethyl siloxane) molecules become more polarized by electric field, leading to higher attraction between the induced electric dipoles on the polythiophene particles and also higher intermolecular interaction between polythiophene particles and PDMS. For the bending response, PTh/PDMS system has better response than pure PDMS in which higher bending angle can be observed. In addition, the bending angle seems to be increased with increasing polythiophene volume fraction and electric field strength.

#### Acknowledgments

The authors wish to thank Associate Prof. Anuvat Sirivat, the Conductive and Electroactive Polymers Research Unit, the Petroleum and Petrochemical College for the assistance of testing equipment and helpful suggestion. D. P. would like to acknowledge the financial support provided by the Thailand Research Fund (TRF-MRG5380100).

#### References

- D. Brandell, H. Kasemagi, A. Aabloo. Electrochimica, 55 (2010), 1333-1337.
- P. Thipdech, R. Kunanuruksapong, A.Sirivat. Express polymer letter vol.2, No.12 (2008), 866-877.
- 3) W. Wichiansee, A. Sirivat. Materials Science and Engineering, 29 (2009), 78–84.
- C. Chuapradit, L. Wannatong, D. Chotpattananont, P. Hiamtup, A. Sirivat, J. Schwank. Polymer, 46 (2005) 947-953.
  - G. G. Wallace, G.M. Spinks, L. Kane-Maguire and P.R. Teasdale. Intelligent materials systems, 2<sup>nd</sup> Edition (2003).
  - D. Zhou, S. Subramaniam, J. E. Mark, Pure and applied chemistry, 42 (2005), 113-126.
  - K. S. Ryu, Y. Lee, K. Seung Han, M. Gyu Kim. Materials chemistry and physics, 84

(2004), 380-384.

- P. Hiamtup, A. Sirivata, A. M. Jamieson. Materials science and engineering, 28 (2008), 1044–1051.
- R. Sakurai, H. See, T. Saito, M. Sumita, J. Non-Newton. Fluid Mech., 81 (1999), 235.

[2] D. Pattavarakorn, K. Jaitang, P. Kumchaiya, P. Chaimongkol and S. Thongbor, "Conductive Polythiophene/Polymer Composites as Electroactive Material Application", 21-26 August 2011, Jeju Island, South Korea.

# CONDUCTIVE POLYTHIOPHENE/POLYMER COMPOSITES AS ELECTROACTIVE MATERIAL APPLICATION

<u>D. Pattavarakorn</u>\*, K. Jaitang, P. Kumchaiya, P. Chaimongkol and S. Thongbor Department of Industrial Chemistry, Faculty of Science, Chiang Mai University, Chiangmai, Thailand

\* Corresponding author (dchpatt@gmail.com, cdatchan@chiangmai.ac.th)

**Keywords**: Electromechanical, Conductive polymer, Polythiophene, PDMS, PVA, Composite

#### Abstract

The conductive polythiophene/poly(dimethyl siloxane), PTh/PDMS composite and polythiophene/polyvinyl alcohol, PTh/PVA composite were prepared in this research. Polythiophene was synthesized via oxidative polymerization in chloroform at 40 °C and then the composites were prepared by mechanical blending of polythiophene particles and polymer fluids. The specified amount of crosslinking agents; tetraethyl orthosilicate, and glutaraldehyde were added for PDMS and PVA composite, respectively. After that, the electromechanical properties; electrorheological properties and bending response under electric field of the composite were investigated. The effects of polythiophene particle concentration (0-30 %vol) and electric field strength (0-2 kV/mm) were studied. The results showed that the composites response well to the electric field. In which, the storage modulus response ( $\Delta G$ ) of the composites increased with the increase in polythiophene particle concentration and electric field strength. For the bending response test under electric field, it was found that the increase electric field strength resulted in the increase of bending angle.

#### Introduction

Electroactive polymers (EAPs) are polymer materials that change their shape or size in response to electrical stimuli. This class of materials is therefore a good candidate for actuators in the field of medical devices, soft manipulators and biomimetics, since they mimic the behavior of biological muscles [1]. The actuators have been produced for many sizes to a variety of styles application. Various materials have been made as actuator: sharp memory alloys (SMA) and electroactive ceramics [2]. However, these materials have limit in terms of weight and ability to change size or sharp. Dielectric elastomers are a type of electric-field-activated electroactive polymers that are capable of producing large strains, fast response. and high efficiency. (dimethylsiloxane) [PDMS], an elastomer, is a potential candidate material for various actuator applications. It has excellent dielectric Properties and flexibility [3]. Currently, conductive polymer (CPs) is alternative to produce for actuators instead of a metallic material. The conductive polymers have many advantages over other material such as low cost,

relatively simple fabrication, light weight and combine the mechanical properties (flexibility, toughness, elasticity, malleability, etc.) of plastics with high electrical conductivities [4], [5]. Many conductive polymers such as polyacetylene, polythiophene, polypyrole, polyaniline have attracted much attention for their promising applications such as sensors, electrochemical displays, batteries, antistatic coatings, anticorrosive coatings, actuator, artificial muscles, functional membranes and controlled release of ionic drugs, etc. [6].

In this study, we are interested to develop polythiophene/polymers composites toward electroactive material application. The electromechanical properties; electrorheological properties and bending response under electric field are investigated in terms of polymer matrix type, polythiophene fraction and electric field strength.

#### Materials

Thiophene (Fluka) was used as the monomer. Iron (III) chloride anhydrous, (Acros organics and Ajax Finechem) was used as the oxidant. Chloroform, (labscan Asia) and methanol (J.T. baker) were used as recieved. Hydroxyl terminated poly(dimethylsiloxane) (PDMS, viscosity 3,500 cSt, Aldrich) and poly(vinyl alcohol) (PVA, Aldrich) were used as matrixes. Tetraethl orthosilicate (TEOS, Aldrich), glutaraldehyde (GA, Aldrich) and dibutyltin dilaurate (2EHSn, Aldrich) were used as crosslinking agents and a catalyst, respectively.

#### Experimental

#### Synthesis of polythiophene (PTh)

was synthesized Polythiophene chemical oxidative polymerization [7]. 145 g of FeCl, anhydrous was added to 800 ml of chloroform and the mixture was stirred in a 3-necked round bottom flask and heat at 40 °C with silicon oil basin. 24.60 g of thiophene monomer (C4H2S) was added to 100 ml of chloroform in a separatory funnel. The thiophene monomer solution was added dropwise to the FeCl<sub>3</sub> anhydrous solution with continuous stirring at room temperature for 3 hours. After all the thiophene monomer solution was added, the reaction mixture was continuity stirred at 40 °C for 9.5 hours and the reaction mixture temperature was decreased to room temperature. After that, 800 ml of methanol was added to the reaction mixture and stirred for 1.5 hour in order to stop the reaction. Polythiophene particles were filtered using Buchner suction funnel and dried in vacuum oven at 27 °C for 24 hours.

# Preparation of PTh/PDMS and PTh/PVA composite films

PTh/PDMS composite films were prepared according to the method of Haimtup et.al. [8]. PTh particles were mixed with HO-PDMS and TEOS at a crosslinking agent to monomer ratio (C/M) of 0.053 using 2EHSn as the catalyst. The mixture was poured in a mold and allowed to cure under vacuum for 24 hours. PTh/PVA composite films were prepared by similar method but GA was used as crosslinking agent and catalyst was not added.

### Electromechanical properties measurement

The electromechanical properties of conductive composites were investigated in the way of electrorheological test and bending response test under the electric field. The effects of polythiophene particle concentration and electric filed strength were studied.

For the electrorheological properties study, composite samples with a diameter of 25 mm and a thickness of 1 mm were prepared. The sample was placed between parallel plates (diameter of 25 mm) of a modified melt rheometer (ARES, Rheometric Scientific Inc.) which is attached to a DC power supply. The samples were first checked for viscoelastic linearity by strain sweep tests. Experiments were carried out in the frequency sweep mode ranging from 0.1 to 100 rad/s to investigate the effect of electric field strength on the storage and loss moduli, G' and G". All experiments at each applied field strengths were repeated twice to confirm reproducibility.

Finally, the bending response of the conductive composites in an electric field was investigated using the experimental set-up as shown in Fig. 1.

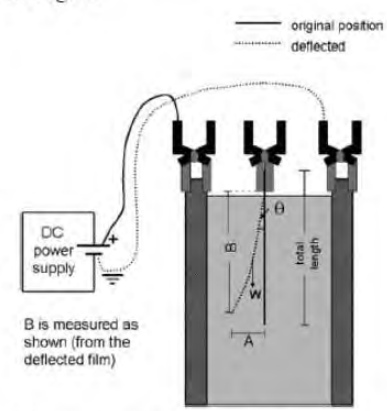


Fig. 1: Schematic diagram of the apparatus used to observe the bending response of the PTh/PDMS blend [8].

The composite films were immersed vertically in a silicon oil (viscosity=100 cSt) bath, with a dc electric field applied horizontally between two parallel flat copper electrodes. DC electric field was applied with various strengths in the range of 0-700 V/mm. The amount of deflection at a specified field strength is defined by the geometrical parameters A, B and  $\theta$ . The bend angle ( $\theta$ ) was calculated from the following equation,

$$\theta = \arctan(A/B)$$
 (2)

#### Results and Discussion

#### Characterization of polythiophene

The FT-IR spectrum of the synthesized polythiophene is showed in Fig. 2. The spectrum shows characteristic peaks at 787 cm<sup>-1</sup>, 1219

cm<sup>-1</sup>, 1367 cm<sup>-1</sup> and 1736 cm<sup>-1</sup> corresponding to the C-C bending vibration, C-C stretching vibration of  $\alpha$ -coupled, C-H stretching vibration and C=C stretching vibration of the thiophene ring, respectively.

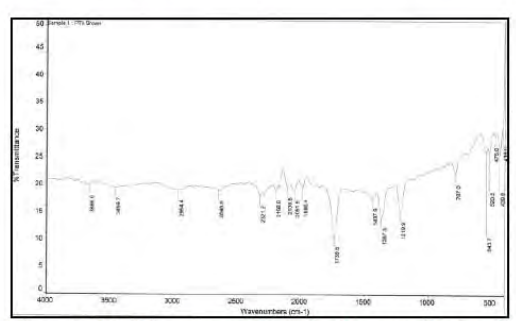


Fig. 2 FT-IR spectrum of the synthesized polythiophene

The UV-Vis absorption spectrum of synthesized polythiophene in DMF solution shows absorption peak at 375 nm and 321 nm, due to the n- $\pi$ \* and  $\pi$ - $\pi$ \* transition of the thiophene unit, respectively. Fig. 4 shows the scanning electron microscopy of synthesized polythiophene particles. It can be seen that the shapes of the polythiophene particles and their surfaces are quite irregular. The specific conductivity of synthesized polythiophene was measured using the two-point probe meter. It was found that the specific conductivity of polythiophene is 8.97 x  $10^{-5}$  S/cm.

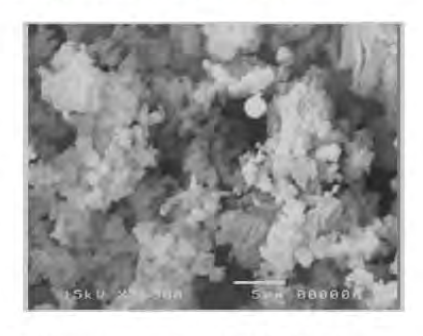


Fig. 3: The morphology of polythiophene.

#### Electrorheological properties of the composites

The effects of particle concentration and electric field strength on electrorheological properties of the composites were explored. Particle volume fraction investigated was varied from 0 to 30 vol. % and the electric field strength was varied as 0-2 kV/mm. The magnitude of the response is characterized as

the difference in storage modulus with the field on  $(G'_E)$  and off  $(G'_{Eo})$ ,  $\Delta G' = G'_E - G'_{Eo}$ , of the composites.

#### - Effect of particle concentration

In PTh/PDMS composite preparation, only blends with polythiophene particle concentration of 0-10 vol. % can be molded. While the composites with higher polythiophene volume fraction crack and cannot be removed from mold. Fig. 4 shows the modulus response of the PTh/PDMS composites as a function of polythiophene particle concentration. It was found that the modulus responses of the PTh/PDMS composites with polythiophene volume fraction less than 5 vol. % are lower than pure PDMS. This might because the crosslink in PDMS is obstructed by polythiophene particles. Moreover, the composite with particle fraction of 5 vol.% showing a trend of greater electromechanical response; at a field strength of 1 kV/mm. The microscopic attraction between the induced electric dipoles on the polythiophene particles evidently causes changes in the overall mechanical properties presumably via an electrostriction effect. The composites with a higher volume fraction have stronger electrostatic interactions, since the average distance between particles is smaller, and these forces increase strongly as the interparticle spacing decreases [9]. In addition, the composite with polythiophene particle of 10 vol.% seems to has lower  $\Delta G'$  than those 5 vol.% composite. This may because of the increase in rigidity of the composite by over electrostatic interaction.

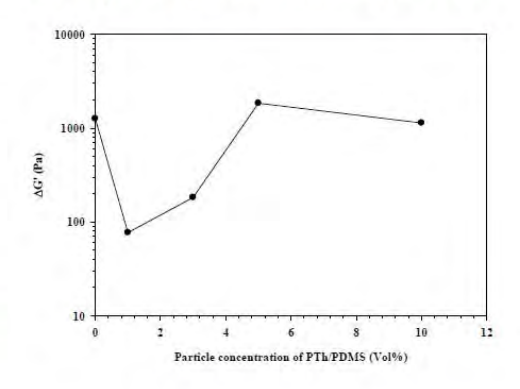


Fig. 4: particle concentration dependence of modulus response  $\Delta G$ ' (at  $\omega=1$  rad/s) of PTh/PDMS blends, measured at E=1 kV/mm and T=27 °C.

#### - Effect of electric field strength

Fig. 5 shows the storage modulus response (ΔG') vs. electric field strength of pure PDMS PTh/PDMS various blend with polythiophene concentrations. It can be seen that the response of each system generally increases with increasing electric field strength. As an electric field is increased, both polythiophene particles and PDMS matrix become more polarize, leading to higher dipole moment and intermolecular interactions. Moreover, the blend with particle fraction 5 vol.% increased marginally with increasing electric field strength due to greater electrostatic interactions as mention above. 2 kV/mm?

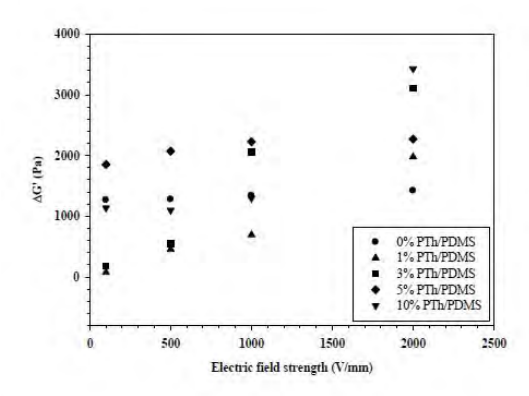


Fig. 5: The storage modulus response ( $\Delta G'$ ) of pure PDMS and PTh/PDMS composites vs. various electric field strengths.

#### Bending response of PTh/PDMS composites

The bending response or deflection of PTh/PDMS composites under electric field was last investigated Fig. 6 shows images of the bending of a PTh/PDMS composites containing 5 vol.% polythiophene particles, immersed in silicone oil at different electric field strengths. The figure shows that on applying the electric field, the free lower end of the composite bends towards the anode by an amount dependent on the field strength. It is indicating an attractive interaction between the applied field and the polarized polythiophene particles in the composites.

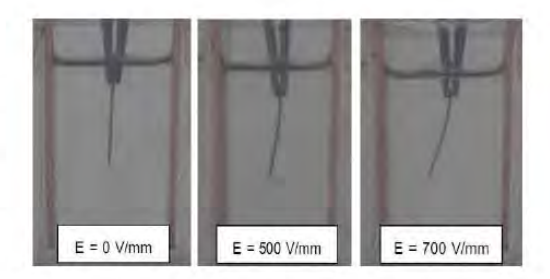


Fig. 6: Bending response of the PTh/PDMS with polythiophene concentration of 5 vol. % at various applied voltages.

The bending angle as a function of polythiophene particle concentration at the field strength of 0.5 kV/mm is shown in Fig. 7. The composites has higher bending angle when the concentration increased. particle PTh/PDMS composite with 10 vol. % polythiophene shows maximum bending angle of 12.53°. The increase in bending angle of PTh/PDMS composites can be attributed to the increase of induced polarization which leading to the increase of interactions between polythiophene particles in PDMS matrix and copper electrode.

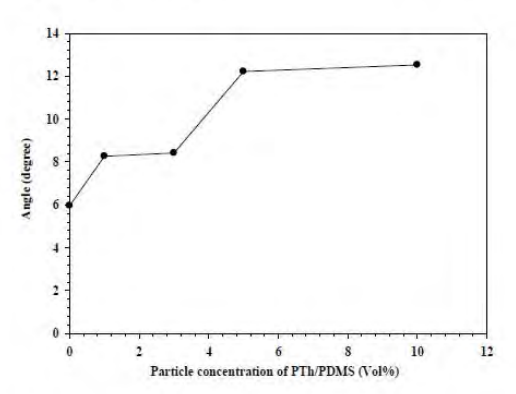


Fig. 7: Bending angle of PTh/PDMS composites with various particle concentrations at electric field strength of 0.5 kV/mm.

Fig. 8 shows the bending angle vs. electric field strength of pure PDMS and 10 vol. % PTh/PDMS composites. The bending response can be observed when applied electric field strength is higher than 0.5 kV/mm for either pure PVDF or 10 vol. % PTh/PDMS sample. The bending angle response appears to increase with increasing of electric field strength, according to greater polarization of polythiophene particles which lead to higher

interaction between polythiophene particle and PDMS matrix.

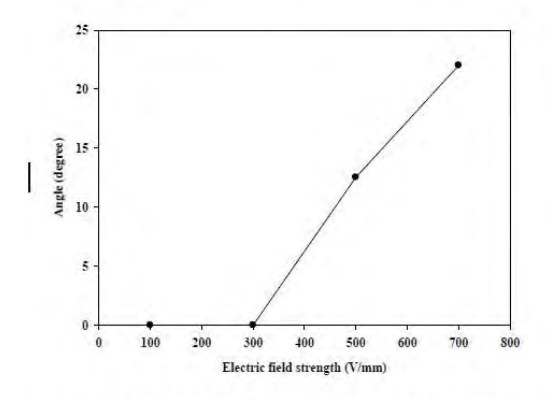


Fig. 8: Bending angle of pure PDMS and 10% PTh/PDMS at various electric field strengths (0, 0.1, 0.3, 0.5 and 0.7 kV/mm).

#### Conclusions

In this study, the electromechanical properties; electrorheological properties and bending response of polythiophene/poly siloxane), PTh/PDMS (dimethyl polythiophene/polyvinyl alcohol, PTh/PVA composites were investigated by examining the effects of polythiophene particle concentration and electric field strength varying from 0 to 2 kV/mm. The storage modulus response (ΔG') increases with particle concentration and electric field strength due to polythiophene particles and poly(dimethyl siloxane) molecules become more polarized by electric field, leading to higher attraction between the induced electric dipoles on the polythiophene particles and also higher intermolecular interaction between polythiophene particles and polymer. For the bending response, PTh/PDMS system has better response than pure PDMS in which higher bending angle can be observed. In addition, the bending angle seems to be increased with increasing polythiophene volume fraction and electric field strength.

#### Acknowledgments

The authors wish to thanks Prof. Anuvat Sirivat, the Conductive and Electroactive Polymers Research Unit, the Petroleum and Petrochemical College for the assistance of testing equipment and we would like to acknowledge the financial support provided by the Thailand Research Fund (TRF-MRG5380100).

#### References

- D. Brandell, H. Kasemagi, A. Aabloo. Electrochimica, 55 (2010), 1333-1337.
- P. Thipdech, R. Kunanuruksapong, A.Sirivat. Express polymer letter vol.2, No.12 (2008), 866-877.
- 3) W. Wichiansee, A. Sirivat. Materials Science and Engineering, 29 (2009), 78–84.
- C. Chuapradit, L. Wannatong, D. Chotpattananont, P. Hiamtup, A. Sirivat, J. Schwank. Polymer, 46 (2005) 947-953.
- G. G. Wallace, G.M. Spinks, L. Kane-Maguire and P.R. Teasdale. Intelligent materials systems, 2<sup>nd</sup> Edition (2003).
- D. Zhou, S. Subramaniam, J. E. Mark, Pure and applied chemistry, 42 (2005), 113-126.
- K. S. Ryu, Y. Lee, K. Seung Han, M. Gyu Kim. Materials chemistry and physics, 84 (2004), 380-384.
- P. Hiamtup, A. Sirivata, A. M. Jamieson. Materials science and engineering, 28 (2008), 1044–1051.
- R. Sakurai, H. See, T. Saito, M. Sumita, J. Non-Newton. Fluid Mech., 81 (1999), 235.

[3] Siripong Thongbor, Siriluck Chumsaratool, Sujitra Thaithed and Datchanee Pattavarakorn, "Electromechanical Properties of Conductive Polythiophene/Poly (dimethyl siloxane) Blend", The 17th Regional Symposium on Chemical Engineering, 22-23 November 2010, Bangkok, Thailand.

 ${\bf TIChE\ International\ Conference\ 2011} \\ {\bf November\ 10-11,\ 2011\ at\ Hatyai,\ Songkhla\ THAILAND}$ 

Paper Code: ms007

### Electromechanical properties of Electroactive Polythiophene/Elastomer Blend

Siripong Thongbor<sup>1</sup>, Datchanee Pattavarakorn<sup>1\*</sup>

Department of Industrial Chemistry, Faculty of Science, Chiang Mai University, Chiangmai, 50200, Thailand \*E-mail: datchanee.p@cmu.ac.th, dchpatt@gmail.com

Abstract – The conductive polythiophene/dielectric elastomer blend was prepared in this research for used as electroactive actuator applications. The poly(dimethyl siloxane) (PDMS) dielectric elastomer was chosen as an elastomer matrix. Conductive polythiophene (PTh) was synthesized via oxidative polymerization in chloroform at 40 °C and then the blend was prepared by mechanical blending of fine PTh particles in PDMS fluid. The specified amount of crosslinking agent; tetraethyl orthosilicate, and catalyst; dibutyltin dilaurate, were added. After that, the electromechanical properties were measured by bending response testing. The effects of polythiophene particle concentration (0-15 vol. %) and electric field strength (0-24 kV/mm) with ratio of crosslinking agent:PDMS of 10, 15, 20 vol. % were studied. The results showed that pure PDMS and PTh/PDMS blends response well to an applied electric field. The bending angle response appears to increase with increasing of polythiophene particle concentration and electric field strength. However, the bending angle decreases with increasing ratio of crosslinking agent:PDMS.

Keywords: Electromechanical, Conductive polymer, Dielectric elastomer, Polythiophene, PDMS

#### **TIChE International Conference 2011**

November 10 - 11, 2011 at Hatyai, Songkhla THAILAND

#### 1. Introduction

Electroactive polymers (EAPs) are polymer materials that change their shape or size in response to electrical stimuli. This class of materials is therefore a good candidate for actuators in the field of medical devices, soft manipulators and biomimetics, since they mimic the behavior of biological muscles [1]. Various materials have been made as actuator; sharp memory alloys (SMA) and electroactive ceramics [2]. However, these materials have limit in terms of weight and ability to change size or sharp. Dielectric elastomers are a type of electric-field-activated electroactive polymers that are capable of producing large strains, fast response, and high efficiency [3]. Currently, conductive polymers (CP) are alternative to produce for actuators instead of a metallic material. The conductive polymers have many advantages over other materials such as low cost, relatively simple fabrication, light weight and combine the mechanical properties (flexibility, toughness, elasticity, malleability, etc.) of plastics with high electrical conductivities [4-6].

In this study, we interest to develop and test the polythiophene/poly (dimethyl siloxane) blend towards actuator applications. The electromechanical properties of the blends are investigated in term of amount of crosslinking agent, polythiophene particle concentration and electric field strength.

#### 2. Experimental

#### 2.1. Materials

Thiophene, C<sub>4</sub>H<sub>2</sub>S (AR grade, Fluka) was used as the monomer. Iron (III) chloride anhydrous, FeCl<sub>3</sub> (AR grade, Carlo Erba) was used as the oxidant. Chloroform, CHCl<sub>3</sub> (AR grade, labscan Asia) and methanol, CH<sub>3</sub>OH (AR grade, J.T. baker) were used as recieved. Hydroxyl terminated poly (dimethylsiloxane), OH-[Si(CH<sub>3</sub>)<sub>2</sub>O]<sub>n</sub>-H (viscosity 3,500 cSt, Aldrich) was used as a elastomeric matrix. Tetraethyl orthosilicate (TEOS), Si (OC<sub>2</sub>H<sub>5</sub>)<sub>4</sub> (AR grade, Aldrich) and dibutyltin dilaurate (2EHSn), [CH<sub>3</sub> (CH<sub>2</sub>)<sub>10</sub>OCO]<sub>2</sub>Sn[(CH<sub>2</sub>)<sub>3</sub>CH<sub>3</sub>]<sub>2</sub> (AR grade, Aldrich) were used as a crosslinking agent and a catalyst, respectively.

#### 2.2. Synthesis of polythiophene (PTh)

Polythiophene was synthesized via chemical oxidative polymerization [7]. FeCl<sub>3</sub> anhydrous was added to chloroform and the mixture was stirred and heat at 40 °C. Thiophene monomer was added to chloroform and then added dropwise to the FeCl<sub>3</sub> solution with continuous stirring at room temperature for 3 hours. After all the thiophene monomer solution was added, the reaction mixture was continuity stirred at 40 °C for 9.5 hours and the reaction was stopped by adding

methanol to the reaction mixture and stirred for 1.5 hour. Polythiophene particles were filtered and dried in vacuum oven at 27  $^{\circ}$ C for 24 hours.

#### 2.3. Preparation of PTh/PDMS blend

The PTh/PDMS blend films were prepared according to the method of W. wichiansee [3]. Polythiphene particles were mixed with PDMS, 2EHSn and TEOS the amount of TEOS was varied as 10, 15 and 20 vol.% (PDMS\_10, PDMS\_15 and PDMS\_20). The mixture was poured in a mold and allowed to cure under vacuum for 24 hours. The volume fraction of polythiophene particle was varied as 5, 10 and 15 vol. % (PTh\_5, PTh\_10, and PTh\_15).

#### 2.4. Electromechanical properties measurement

The electromechanical properties of the PTh/PDMS blend were investigated in the way of the bending response. The experimental setup as show in "Fig.1". The samples were vertically immersed in silicon oil (viscosity=100 CSt) with a dc electric field applied between two copper electrodes (30 mm long, 30 mm wide, and 1.0 mm in thickness; the distance between the electrodes is 30 mm). All of experiments were recorded by video camera and the amount of deflection bending angle ( $\theta$ ) was calculated from the following equation,

 $\theta$  = arctan (A/B) (1) where A is the measured deflection distance and B is the sample length. Which were detected by Engauge

Digitizer (4.1) program.

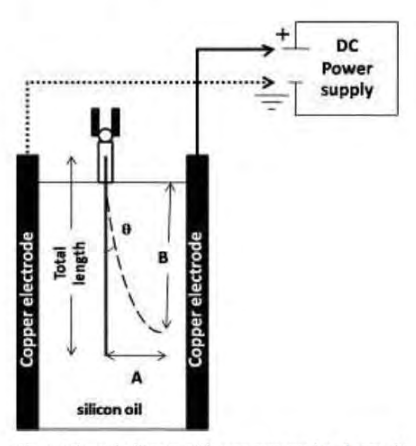


Fig. 1. Schematic diagram of the apparatus used to observe the

#### **TIChE International Conference 2011**

November 10 - 11, 2011 at Hatyai, Songkhla THAILAND

#### 3. Results and Discussion

#### 3.1. Appearance of PTh/PDMS blends

The blend was prepared by mechanical mixing sieved polythiophene with poly(dimethyl siloxane) and then blend film was prepared by solution casting. "Fig.2" shows images of the appearance of PTh/PDMS blend films, diameter is 80 mm and thickness is approximately 0.8 mm, containing 5 vol.% PTh particles. The surface of pure PDMS film appears generally transparent, smooth and shiny. It is soft and smooth surface and lower flexibility can be observed. This indicated that polythiophene particles act as reinforcing filler to PDMS matrix.

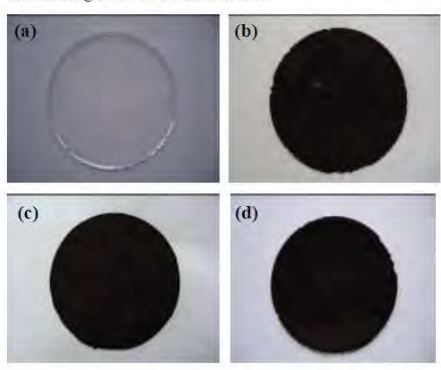


Fig. 2. The PTh/PDMS blend samples at various PTh particle concentrations; (a) pure PDMS \_10, (b) PTh\_5/PDMS\_10, (c) PTh\_10/PDMS\_10 and (d) PTh\_15/PDMS\_10.

#### 3.2. Bending response

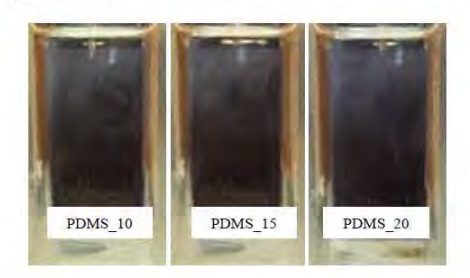
The bending response or deflections of the PTh/PDMS blends samples were recorded using video camera and the bending response angle was calculated using equation (1). Under an application of electric field, the free lower end of the blends bend toward an anode electrode by an amount dependent on the studied variables; amount of crosslink agent, PTh particle concentration and electric field strength. In addition, the blends suddenly return approximately to original position when the electric field is removed.

#### 3.2.1 Effect of amount of crosslinking agent

The effect of crosslink on the bending response of the pure PDMS and PTh/PDMS blend were investigated. The amount of TEOS crosslink agent was varied as 10%, 15% and 20 vol% (PDMS\_10, PDMS\_15 and PDMS\_20). The bending response and the bending angle of the PDMS and PTh/PDMS blend samples at electric field strength of 400 V/nm are shown in "Fig. 3" and "Fig. 4", respectively. It was found that the

bending angle decreases with increasing amount of crosslink agent in which the bending angles of PDMS\_10, PDMS\_15 and PDMS\_20 are 50.24, 36.34 and 9.84, respectively. This may because the crosslinking agent prohibits the free movement of PDMS chains and consequently leading to decreasing in the interaction between PDMS matrix, therefore the PDMS characteristic changes to more solid-like behavior [8]. Moreover, with the addition of PTh particles results in the decrease of the response angle. Similar to the PDMS system, the bending angle of the PTh\_5/PDMS blend system decreases with the increase of the amount of crosslink agent.

#### (a) PDMS



#### (b) PTh 5/PDMS blends



Fig. 3. Bending response pictures of PTh/PDMS blends at electric field strength of 400 V/mm; (a) PDMS and (b) 5%vol. PTh/PDMS blends

# TIChE International Conference 2011 November 10-11, 2011 at Hatyai, Songkhla THAILAND

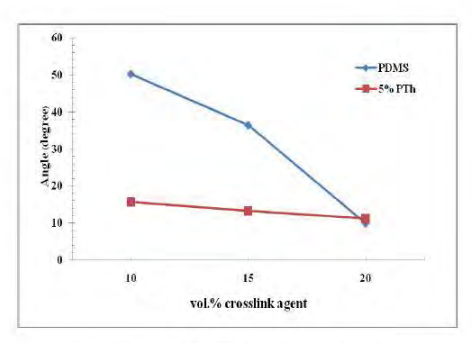


Fig. 4. Bending angle of the PDMS and PTh\_5/PDMS blend vs. amount of crosslink agent at electric field strength of 400 V/mm

#### 3.2.2 Effect of PTh particle concentration

The effect of particle concentration on the bending response of the PTh/PDMS blend was investigated by varying the polythiophene particle concentration as 5, 10 and 15 vol. % (PTh\_5, PTh\_10, and PTh\_15). The bending response and the bending angle of the PDMS and PTh/PDMS blend samples at electric field strength of 233 V/mm are shown in "Fig. 5" and "Fig. 6", respectively. From "Fig. 6", it can be observed that the pure PDMS has higher bending angle than PTh/PDMS blends, suggesting a higher flexibility. Moreover, bending angle of the PTh/PDMS blend linearly increases with PTh particle concentration, indicating an attractive interaction between the applied field and polarized polythiophene particles in PDMS matrix.

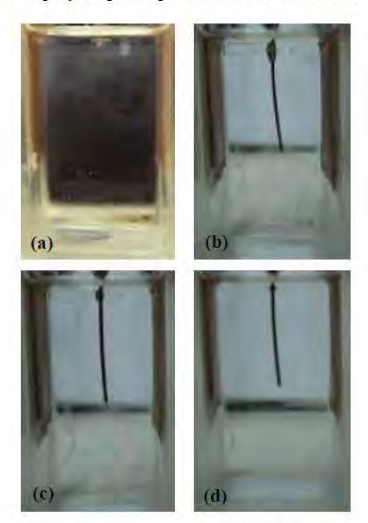


Fig. 5. Bending response pictures of a PTh/PDMS blends at electric field strength of 233 V/mm; (a) PDMS\_10, (b) PTh\_5/PDMS\_10, (c) PTh\_10/PDMS\_10 and (d) PTh\_15/PDMS\_10 blends.

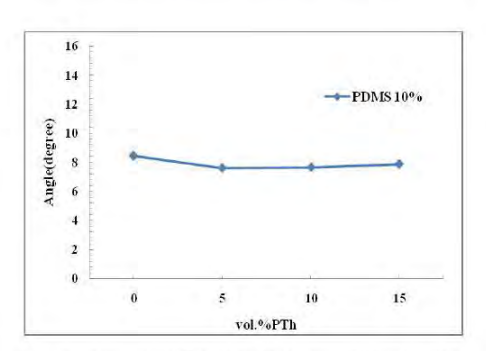


Fig. 6. Bending angle of PTh/PDMS\_10 blend vs. vol.% PTh particles at electric field atrength of 233 V/mm.

#### 3.2.3 Effect of electric field strength

The bending response and the bending angle of the PDMS and PTh/PDMS blend samples at electric field strength of 233 V/mm are shown in "Fig. 7" and "Fig. 8", respectively. "Fig.8" shows that the bending angle of the PDMS and PTh/PDMS blend appears to increase monotonically with electric field strength. As electric field is applied, electrical dipole moments are generated and leads to the attractive interaction between the applied field and the polarized polythiophene particles in the blend. With higher electric field strength, higher polarization and dipole interaction strongly effect to the increase of bending angle of the blend [9].

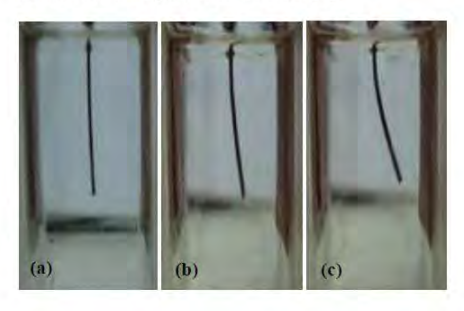


Fig. 7. Bending response pictures of PTh\_15/PDMS\_10 blend at electric field strengths of; (a) 0 V/mm, (b) 400 V/mm and (c) 800 V/mm.

**TIChE International Conference 2011** November 10 - 11, 2011 at Hatyai, Songkhla THAILAND

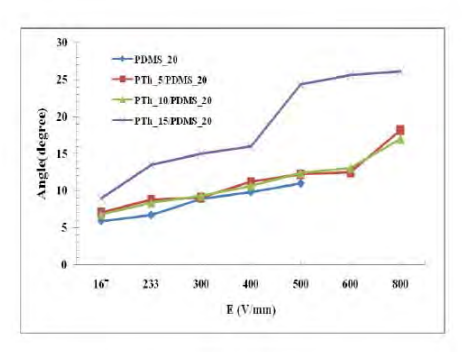


Fig. 8. Bending angle of PDMS\_20 and PTh/PDMS\_20 blends vs. electric field strength.

#### 4 Conclusions

In this study, the bending response of PTh/PDMS was investigated by examining the effect of the amount of crosslink agent, polythiophene particle concentration and an electric field strength. In pure PDMS system, the bending angle decreased with increasing crosslink ratio. The maximum bending angle was found to be 50.24 for the PDMS\_10. For the blending response of the PTh/PDMS blend, it was found that the bending angle increased with increasing of polythiophene particle concentration and electric field strength within the range because the poly(dimethyl siloxane) and polythiophene particle were polarized and electrical dipole moments are generated. These lead to the attractive interaction between the applied field and the polarized polythiophene particles in the blend.

#### Acknowledgement

The authors would like to acknowledge the financial supports provided by the Thailand Research Fund (MRG5380100) and the faculty of Science, Chiang Mai University.

#### References

- [1] D.Brandell, H. Kasemagi, A. Aabloo. Electrochimica, 55
- [2]
- D.Brancell, H. Kasemagi, A. Aaoloo. Electrochimica, 55 (2010), 1333-1337.

  P. Thipdech, R. Kunanuruksapong, A.Sirivat. Express polymer letter vol.2, No.12 (2008), 866-877.

  W. Wichiansee, A. Sirivat. Materials Science and Engineering, 2000, 2000, 2004.
- 29 (2009), 78–84. C. Chuapradit, L. Wannatong, D. Chotpattananont, P. Hiamtup,
- [4]

- C. Chuapradit, L. Wannatong, D. Chotpattananont, P. Hiamtup, A. Sirivat, J. Schwank. Polymer, 46 (2005) 947-953.
  G. Wallace, G.M. Spinks, L. Kane-Maguire and P.R. Teasdale. Intelligent materials systems, 2nd Edition (2003).
  D. Zhou, S. Subramaniam, J. E. Mark, Pure and applied chemistry, 42 (2005), 113-126.
  K. S. Ryu, Y. Lee, K. Seung Han, M. Gyu Kim. Materials chemistry and physics, 84 (2004), 380-384.
  T. Puvanatvattana, D. chotpattananont, P. Hiamtup, S. Niamlang, A. Sirivat, A.M. Jamieson. Reactive & Functional Polymers, 66 (2006), 1575-1588.

[9] P. Hiamtup, A. Sirivat, A. M. Jamieson. Materials Science and Engineering, 28 (2008), 1044-1051.